Molecular Therapy
Nucleic Acids
Original Article

Role of linc00174/miR-138-5p (miR-150-5p)/FOSL2 Feedback Loop on Regulating the Blood-Tumor Barrier Permeability

Jizhe Guo,[1,2,3,7] Shuyuan Shen,[1,2,3,7] Xiaobai Liu,[4,5,6,7] Xuelei Ruan,[1,2,3,7] Jian Zheng,[4,5,6] Yunhui Liu,[4,5,6] Libo Liu,[1,2,3] Jun Ma,[1,2,3] Teng Ma,[1,2,3] Lianqi Shao,[1,2,3] Di Wang,[4,5,6] Chunqing Yang,[4,5,6] and Yixue Xue[1,2,3]

[1]Department of Neurobiology, School of Life Sciences, China Medical University, Shenyang 110122, People's Republic of China; [2]Key Laboratory of Cell Biology, Ministry of Public Health of China, China Medical University, Shenyang 110122, People's Republic of China; [3]Key Laboratory of Medical Cell Biology, Ministry of Education of China, China Medical University, Shenyang 110122, People's Republic of China; [4]Department of Neurosurgery, Shengjing Hospital of China Medical University, Shenyang 110004, People's Republic of China; [5]Liaoning Research Center for Translational Medicine in Nervous System Disease, Shenyang 110004, People's Republic of China; [6]Key Laboratory of Neuro-oncology in Liaoning Province, Shenyang 110004, People's Republic of China

The blood-tumor barrier (BTB) limits the transport of chemotherapeutic drugs to brain tumor tissues and impacts the treatment of glioma. Long non-coding RNAs play critical roles in various biological processes of tumors; however, the function of these in BTB permeability is still unclear. In this study, we have identified that long intergenic non-protein coding RNA 174 (linc00174) was upregulated in glioma endothelial cells (GECs) from glioma tissues. Additionally, linc00174 was also upregulated in GECs from the BTB model *in vitro*. Knock down of linc00174 increased BTB permeability and reduced the expression of the tight junction-related proteins ZO-1, occludin, and claudin-5. Both bioinformatics data and results of luciferase reporter assays demonstrated that linc00174 regulated BTB permeability by binding to miR-138-5p and miR-150-5p. Furthermore, knock down of linc00174 inhibited FOSL2 expression via upregulating miR-138-5p and miR-150-5p. FOSL2 interacted with the promoter regions and upregulated the promoter activity of ZO-1, occludin, claudin-5, and linc00174 in GECs. In conclusion, the present study demonstrated that the linc00174/miR-138-5p (miR-150-5p)/FOSL2 feedback loop played an essential role in regulating BTB permeability.

INTRODUCTION

Glioma is the most common primary malignant tumor in the CNS.[1] Despite that surgical treatment combined with postoperative chemotherapy is the most effective treatment at present, the prognosis is poor in patients suffering from glioma.[2] Chemotherapy is one of the most important methods in the treatment of glioma. Because the blood-tumor barrier (BTB) greatly limits the entry of most antitumor drugs into tumor tissues, the effectiveness of chemotherapy for glioma is reduced. Therefore, selective opening of the BTB, as well as increasing transporting drugs into glioma tissues, is one of the most important parts in improving the chemotherapeutic effect of glioma.

Similar to the blood-brain barrier (BBB), the BTB is mainly composed of brain microvascular endothelial cells (BMECs), basal membranes, and glioma cells.[3] There are two main routes for drugs to reach tumor tissues via the BTB, including the paracellular pathway and the transcellular pathway.[4] The paracellular pathway involves the opening up of the tight junctions among endothelial cells (ECs), and tight junctions are mainly composed of gaps or fusion channels between tight junctions consisting of tight junction-associated proteins such as zonula occludens proteins (ZOs), occludin, and claudins.[5]

Abundant and functionally important types of non-coding RNAs include long non-coding RNAs (lncRNAs), as well as short non-coding RNAs, such as microRNAs (miRNAs), small interfering RNAs (siRNAs), PIWI-interacting RNAs (piRNAs), small nucleolar RNAs (snoRNAs), and others. Recent studies have shown that lncRNAs play important roles in the regulation of tumors and inflammatory, neurodegenerative, and other diseases.[6] Molecular regulatory networks centered on lncRNAs regulating BTB permeability have attracted great attention of researchers. lncRNAs are RNAs with a length of more than 200 nt that have no capacity to code for protein due to the lack of an open reading frame.[7] lncRNAs regulate the expression of target genes at the levels of transcription, post-transcription, and epigenetics.[8] Long intergenic non-protein coding RNA 174 (linc00174) is located on chromosome 7q11.21. However, the regulation of GECs function by linc00174 has not been investigated.

miRNAs, about 22 nt in length, regulate the expression of target mRNA by binding to the 3′ UTR of complementary target mRNA completely or incompletely.[9] miR-138-5p is a member of the

Received 14 April 2019; accepted 26 October 2019;
https://doi.org/10.1016/j.omtn.2019.10.031.

[7]These authors contributed equally to this work.

Correspondence: Yixue Xue, Department of Neurobiology, College of Life Sciences, China Medical University, Shenyang 110122, People's Republic of China.
E-mail: xueyixue888@163.com

miR-138 family, which contains a 23-bp sequence locus on chromosome 16, and is involved in modulating biological behaviors of multiple tumor cells. miR-138-5p was reported to be downregulated in the tissues and cells of melanoma[10] and renal cell carcinoma,[11] and it participated in the regulation of cancer development and progression. miR-150-5p, located on chromosome 19 with a length of 22 bp, showed a low expression level in colorectal cancer, non-small cell lung cancer, and other tumors, while inhibiting the proliferation, migration, and invasion of the above tumor cells.[12,13] At present, no studies on the regulation of BTB function by miR-138-5p and miR-150-5p have been reported.

FOSL2 also known as FRA2, belongs to the activator protein-1 (AP1) transcription factors family, which includes the various isoforms of Fos and Jun.[14,15] The leucine chain encoded by the Fos gene can dimerize with the protein encoded by the Jun gene family (including C-Jun, JunB, and JunD) to synthesize into AP1. AP1 is involved in the regulation of cell proliferation, differentiation, and transformation, as well as embryonic development,[16] organogenesis,[17] and immune system regulation.[18] Studies have shown that FOSL2 participates in the regulation of physiological and pathological processes in a variety of cells. FOSL2 specifically expressed in osteoblasts regulates adiponectin and osteocalcin expression and metabolism.[19] FOSL2 is involved in regulation of the photoperiod in the pineal gland[20] and promotes myocardial fibrosis.[21] FOSL2 promotes the progression of ovarian precancerous lesions.[22] In addition, FOSL2 is highly expressed in breast cancer cells and promotes the proliferation, migration, and invasion of breast cancer.[23] However, the regulation of BTB function by FOSL2 remains unclear.

In the present study, we first verified the endogenous expression of linc00174, miR-138-5p, miR-150-5p, and FOSL2 in glioma microvascular endothelium and the effect of these molecules on the permeability of BTB. Furthermore, we investigated the regulatory relationship and mechanisms of these molecules, as well as their key points in regulating the permeability of BTB. This study aims to reveal the new mechanism for regulating the permeability of BTB, while also providing new ideas for the comprehensive therapy of glioma.

RESULTS

Inhibition of linc00174 Increased BTB Permeability and Decreased the Expression Levels of Tight Junction-Related Proteins in GECs

The expression of linc00174 in the astrocytes-endothelial cells (AECs) and GECs was evaluated. As shown in Figures 1A and 1C, lncRNA microarrays and quantitative real-time PCR were performed and results showed that the expression of linc00174 in GECs was significantly higher than that in AECs. To explore the possible functional role of linc00174 on BTB permeability, GECs with stable knock down of linc00174 were established. Therefore, transendothelial electric resistance (TEER) values were detected. There was no significant difference in TEER values between the control group and the linc00174(−) negative control (NC) group. TEER values were significantly decreased in the linc00174(−) group compared with that in the linc00174(−)NC group, which suggested that linc00174 knockdown impaired the BTB integrity (Figure 1D). As shown in Figure 1E, the horseradish peroxidase (HRP) flux was much higher in the linc00174(−) group than that in linc00174(−)NC group, indicating that linc00174 inhibition increased the permeability of BTB. To further verify the potential mechanisms of linc00174 on BTB permeability, the expression of ZO-1, occludin, and claudin-5 was detected by western blot. Figure 1F shows no significant difference between control and linc00174(−)NC groups. However, the expressions of ZO-1, occludin, and claudin-5 were decreased in linc00174(−) group compared with the lin00174(−)NC group. Similar to the results of western blot, the immunofluorescence staining results revealed that, compared with the linc00174(−)NC group, the expressions of ZO-1, occludin, and claudin-5 were significantly decreased in the linc00174(−) group and exhibited a discontinuous distribution (Figure 1G).

Overexpression of miR-138-5p or miR-150-5p Increased BTB Permeability and Decreased the Expressions of ZO-1, Occludin, and Claudin-5 in GECs

Quantitative real-time PCR were performed to detect the expression levels of miR-138-5p and miR-150-5p in GECs. Figures 2A and 2F showed that the expressions of miR-138-5p and miR-150-5p were significantly decreased in the GECs group compared with that in the AECs group. To further clarify the effect of miR-138-5p and miR-150-5p on BTB permeability, overexpression and inhibition of miR-138-5p or miR-150-5p, respectively, were transiently transfected in GECs. TEER values were detected. The TEER values were significant decreased in the miR-138-5p(+) or miR-150-5p(+) group compared with the miR-138-5p(+)NC or miR-150-5p(+)NC group, whereas the TEER values were increased in miR-138-5p(−) or miR-150-5p(−) group compared with miR-138-5p(−)NC or miR-150-5p(−)NC group (Figures 2B and 2G). However, the HRP flux in the miR-138-5p(+) or miR-150-5p(+) group was significantly higher than that in the miR-138-5p(+)NC or miR-150-5p(+)NC group. The HRP flux in the miR-138-5p(−) or miR-150-5p(−) group was significantly lower than that in miR-138-5p(−) or miR-150-5p(−) group (Figures 2C and 2H). These results demonstrated that overexpression of miR-138-5p or miR-150-5p increased the BTB permeability in GECs. Furthermore, western blot was conducted to clarify the potential mechanism in the changes of BTB permeability. As shown in Figures 2D and 2I, the expression of ZO-1, occludin, and claudin-5 were significantly decreased in the miR-138-5p(+) or miR-150-5p(+) group compared with the miR-138-5p(+)NC or miR-150-5p(+)NC group. Those proteins were significantly increased in the miR-138-5p(−) or miR-150-5p(−) group. As shown in Figures 2E and 2J, the effects of miR-138-5p or miR-150-5p overexpression on ZO-1, occludin, and claudin-5 protein levels and distribution were determined via immunofluorescence staining. However, discontinuous distribution and downregulation of expression of these tight junction-related proteins were determined. The opposite results were observed in the miR-138-5p(−) or miR-150-5p(−) group.

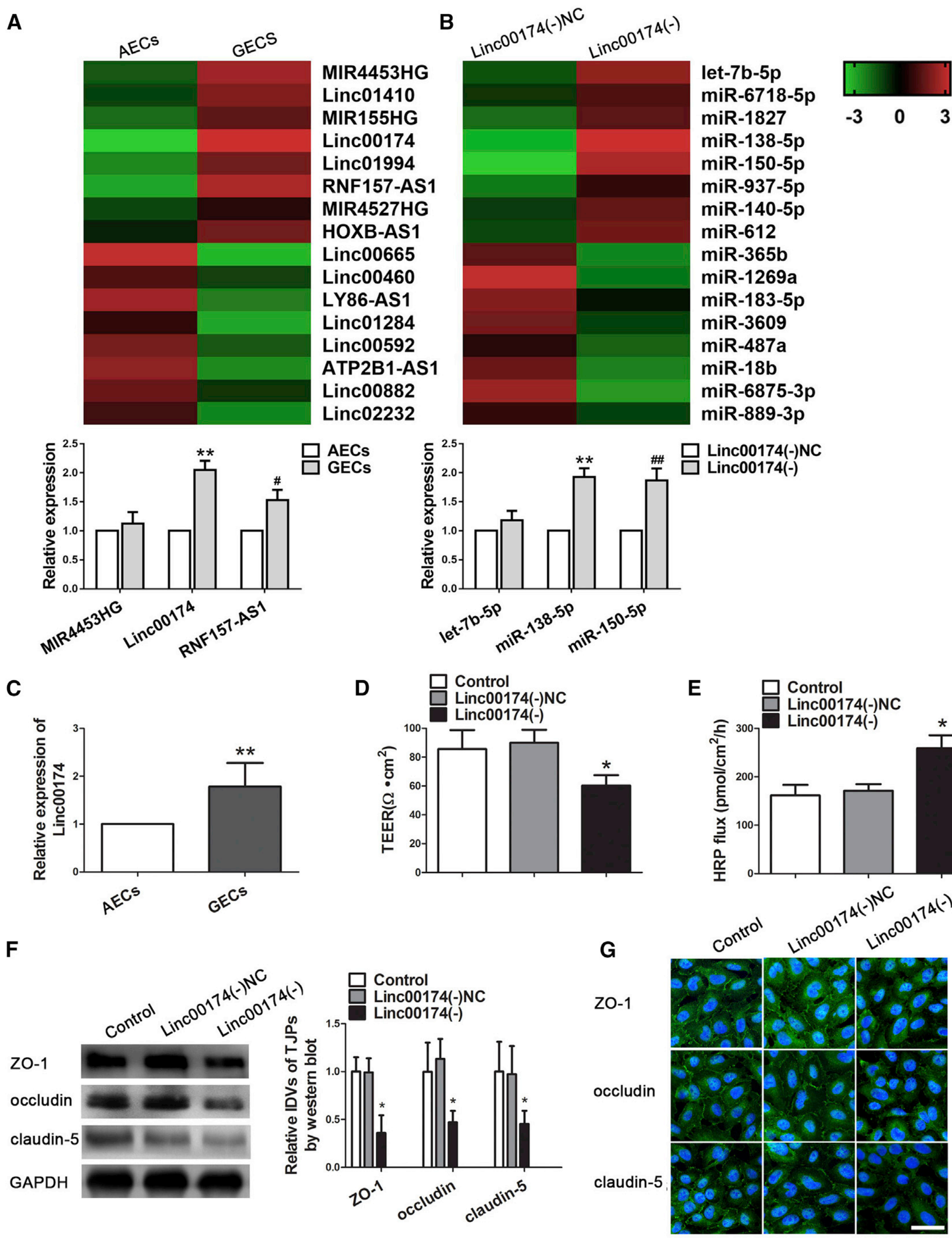

Figure 1. linc00174 Was Highly Expressed in GECs, and Knock Down of linc00174 Increased BTB Permeability and Induced the Expression of Tight Junction-Related Proteins in GECs

(A and B) lncRNA (A) and miRNA (B) microarray data in AECs and GECs; quantitative real-time PCR were performed to validate the selected molecules. (C) Relative expression levels of linc00174 in AECs and GECs were detected by quantitative real-time PCR. Data represent mean ± SD (n = 5, each). $^{**}p < 0.01$ versus AECs group. (D) TEER values were evaluated after knock down of linc00174 in GECs. (E) HRP flux assays were performed to detect permeability after knock down of linc00174 in GECs. Data represent mean ± SD (n = 5, each). $^{*}p < 0.05$ versus linc00174(−) group. (F) Western blot analysis for the protein expression of tight junction-related proteins ZO-1, occludin, and claudin-5 in GECs. Data represent mean ± SD (n = 3, each). $^{*}p < 0.05$ versus linc00174(−) group. (G) Immunofluorescence localization of ZO-1, occludin, and claudin-5 in GECs. Nuclei are labeled with DAPI. Images are representative of three independent experiments. Scale bar, 50 μm.

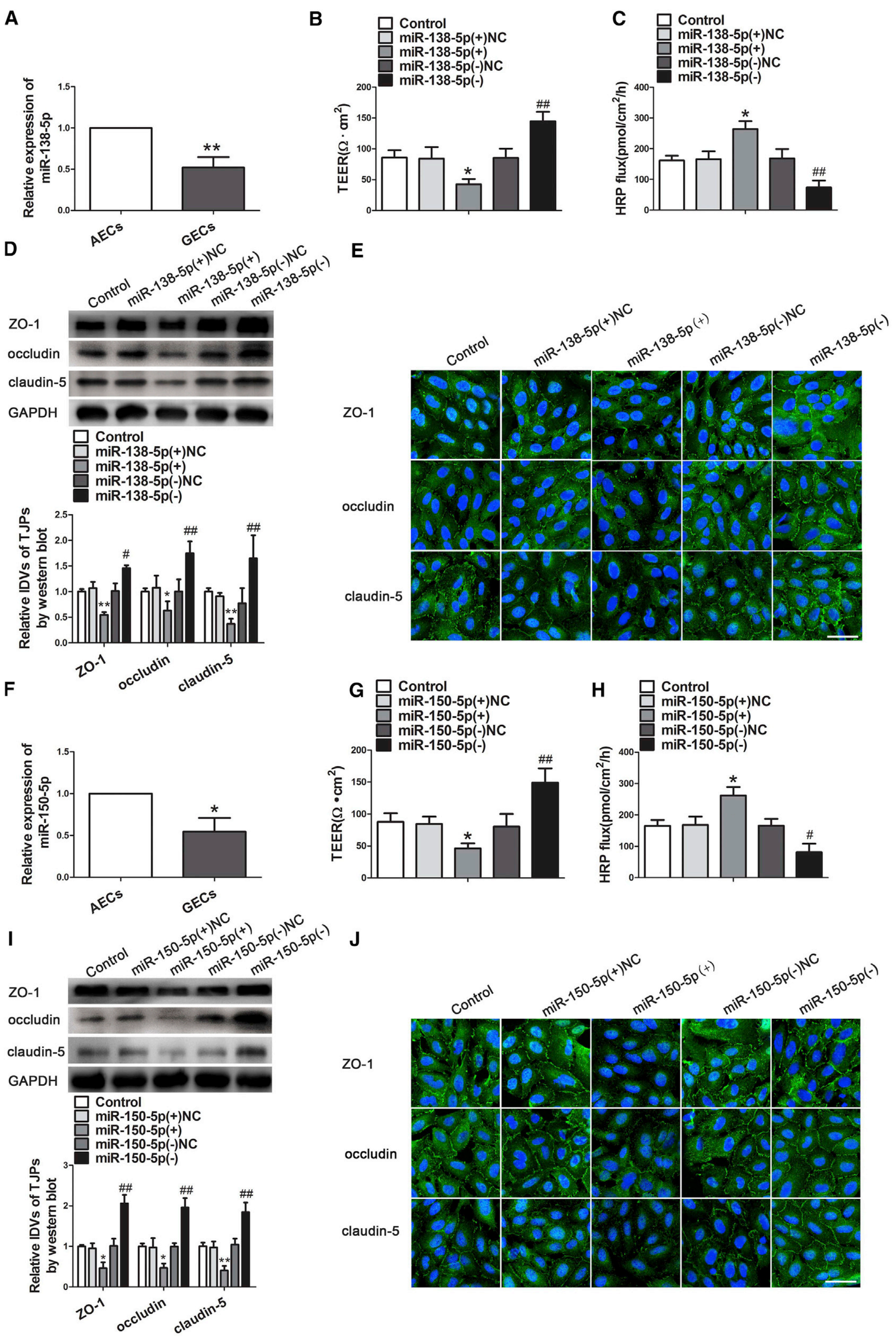

(legend on next page)

linc00174 Bound to miR-138-5p and miR-150-5p, linc00174 and miR-138-5p, or miR-150-5p Were Reciprocally Repressed

Database: starBase v2.0 was used to detect whether linc00174 has a potential binding site on miR-138-5p and miR-150-5p. As Figure 1B shows, miRNA microarrays and quantitative real-time PCR were performed to screen the target miRNAs with linc00174 inhibition. Meanwhile, Figures 3A and 3H showed that the expressions of miR-138-5p and miR-150-5p were significantly increased after stable knock down of linc00174. However, linc00174 expression was decreased in the miR-138-5p(+) or miR-150-5p(+) group and increased in the miR-138-5p(−) or miR-150-5p(−) group (Figures 3B and 3I). The above results indicated that linc00174 and miR-138-5p or miR-150-5p were reciprocally repressed. Furthermore, a luciferase reporter assay was performed. Luciferase activity was not significantly different in cells co-transfected with miR-138-5p(+) or miR-150-5p(+) and linc00174-Mut. However, luciferase activity was significantly decreased in cells co-transfected in miR-138-5p(+) or miR-150-5p(+) and linc00174-wild-type (Wt) (Figures 3C and 3J). An RNA immunoprecipitation (RIP) assay was performed and showed that the enrichment of linc00174 and miR-138-5p or miR-150-5p was higher in the anti-Ago2 group than that in the anti-normal immunoglobulin G (IgG) group. However, knock down of miR-138-5p or miR-150-5p reduced the enrichment of linc00174 and miR-138-5p or miR-150-5p in Ago2 precipitates (Figures 3D and 3K).

miR-138-5p and miR-150-5p Mediate linc00174-Regulated BTB Permeability

Having confirmed that miR-138-5p and miR-150-5p were negatively regulated by linc00174, we further speculated that miR-138-5p and miR-150-5p might be involved in the effects of linc00174 knockdown on BTB permeability. Overexpression or knockdown of miR-138-5p or miR-150-5p was co-transfected in GECs with linc00174 inhibition. As shown in Figures 3E and 3L, TEER values were significant decreased in the GECs with miR-138-5p or miR-150-5p overexpression, which stably knocked down linc00174. However, miR-138-5p or miR-150-5p inhibition, which stably knocked down linc00174, largely rescued the inhibition effect of linc00174(−) on TEER values. Similarly, miR-138-5p or miR-150-5p inhibition, which stably knocked down linc00174, largely rescued the promotion effect of linc00174(−) on HRP flux (Figures 3F and 3M). In addition, the protein expressions of ZO-1, occludin, and claudin-5 were detected by western blot. The expressions of ZO-1, occludin, and claudin-5 were decreased after overexpression of miR-138-5p or miR-150-5p, which stably knocked down linc00174. However, miR-138-5p or miR-150-5p inhibition, which stably knocked down linc00174, largely rescued the inhibition effect of linc00174(−) on ZO-1, occludin, and claudin-5 expression (Figures 3G and 3N).

FOSL2 Was Upregulated in GECs, and Knock Down of FOSL2 Increased the BTB Permeability while Decreasing the Expression of ZO-1, Occludin, and Claudin-5

In this study, quantitative real-time PCR and western blot assays were used to detect the expression of transcription factor FOSL2 in AECs and GECs. As shown in Figures 4A and 4B, both mRNA and protein expressions of FOSL2 were increased in GECs, compared with AECs. To further clarify the functional role of FOSL2 in GECs, we established stable GEC cell lines with overexpression or inhibition of FOSL2. Figures 4C and 4D showed that FOSL2 overexpression increased the TEER values, whereas it decreased HRP flux, compared with the FOSL2(+)NC group. However, FOSL2 knockdown decreased the TEER values, whereas it increased HRP flux, compared with the FOSL2(−)NC group. These results demonstrated that FOSL2 inhibition promoted BTB permeability. Furthermore, the mRNA and protein expressions of ZO-1, occludin, and claudin-5 were detected by quantitative real-time PCR and western blot. Both mRNA and protein expression were increased in the FOSL2(+) group, compared with the FOSL2(+)NC group, whereas it decreased in the FOSL2(−) group compared with the FOSL2(−)NC group (Figures 4E and 4F). Similar to western blot, immunofluorescence staining revealed that ZO-1, occludin, and claudin-5 exhibited a discontinuous distribution and decrease in the FOSL2(−) group compared with the FOSL2(−)NC group. However, the opposite results were shown in the FOSL2(+) group (Figure 4G).

Both miR-138-5p and miR-150-5p Targeted the FOSL2 3′ UTR

In this study, having confirmed that FOSL2 played an oncogenic role in GECs, we further detected whether FOSL2 was involved in linc00174-downregulated, induced regulation of BTB permeability. As shown in Figures 5A and 5B, both mRNA and protein expressions of FOSL2 were significantly decreased in the linc00174(−) group, compared with the linc00174(−)NC group. Furthermore, we assessed the effects of miR-138-5p or miR-150-5p overexpression and inhibition on the expression of FOSL2. Figures 5C–5F show that

Figure 2. miR-138-5p and miR-150-5p Regulate BTB Permeability and the Expression of Tight Junction-Related Proteins in GECs

(A) Relative expression levels of miR-138-5p were detected by quantitative real-time PCR in AECs or GECs. Data represent mean ± SD (n = 3, each). $^{**}p < 0.01$ versus AECs group. (B) TEER values of BTB were detected after overexpression and inhibition of miR-138-5p in GECs. (C) HRP flux assay was performed to detect BTB permeability. Data represent mean ± SD (n = 5, each). $^{*}p < 0.05$ versus miR-138-5p(+)NC; $^{\#\#}p < 0.01$ versus miR-138-5p(−)NC. (D) Western blot analysis of ZO-1, occludin, and claudin-5 in GECs. Data represent mean ± SD (n = 3, each). $^{*}p < 0.05$ and $^{**}p < 0.01$ versus miR-138-5p(+)NC; $^{\#}p < 0.05$ and $^{\#\#}p < 0.01$ versus miR-138-5p(−)NC. (E) Immunofluorescence localization of ZO-1, occludin, and claudin-5 in GECs. Nuclei are labeled with DAPI. Images are representative of three independent experiments. Scale bar, 50 μm. (F) Relative expression levels of miR-150-5p were detected by quantitative real-time PCR in AECs or GECs. Data represent mean ± SD (n = 3, each). $^{*}p < 0.05$ versus AECs group. (G) TEER values were detected on BTB integrity, after overexpression and inhibition of miR-150-5p in GECs. (H) HRP flux assay was performed to detect BTB permeability. Data represent mean ± SD (n = 5, each). $^{*}p < 0.05$ versus miR-150-5p(+)NC; $^{\#}p < 0.05$ and $^{\#\#}p < 0.01$ versus miR-150-5p(−)NC. (I) Western blot analysis expression of ZO-1, occludin, and claudin-5 after transfection of miR-150-5p mimics and inhibitor in GECs. Data represent mean ± SD (n = 3, each). $^{*}p < 0.05$ and $^{**}p < 0.01$ versus miR-150-5p(+)NC; $^{\#\#}p < 0.01$ versus miR-150-5p(−)NC. (J) Immunofluorescence localization of ZO-1, occludin, and claudin-5 in GECs. Nuclei are labeled with DAPI. Images are representative of three independent experiments. Scale bar, 50 μm.

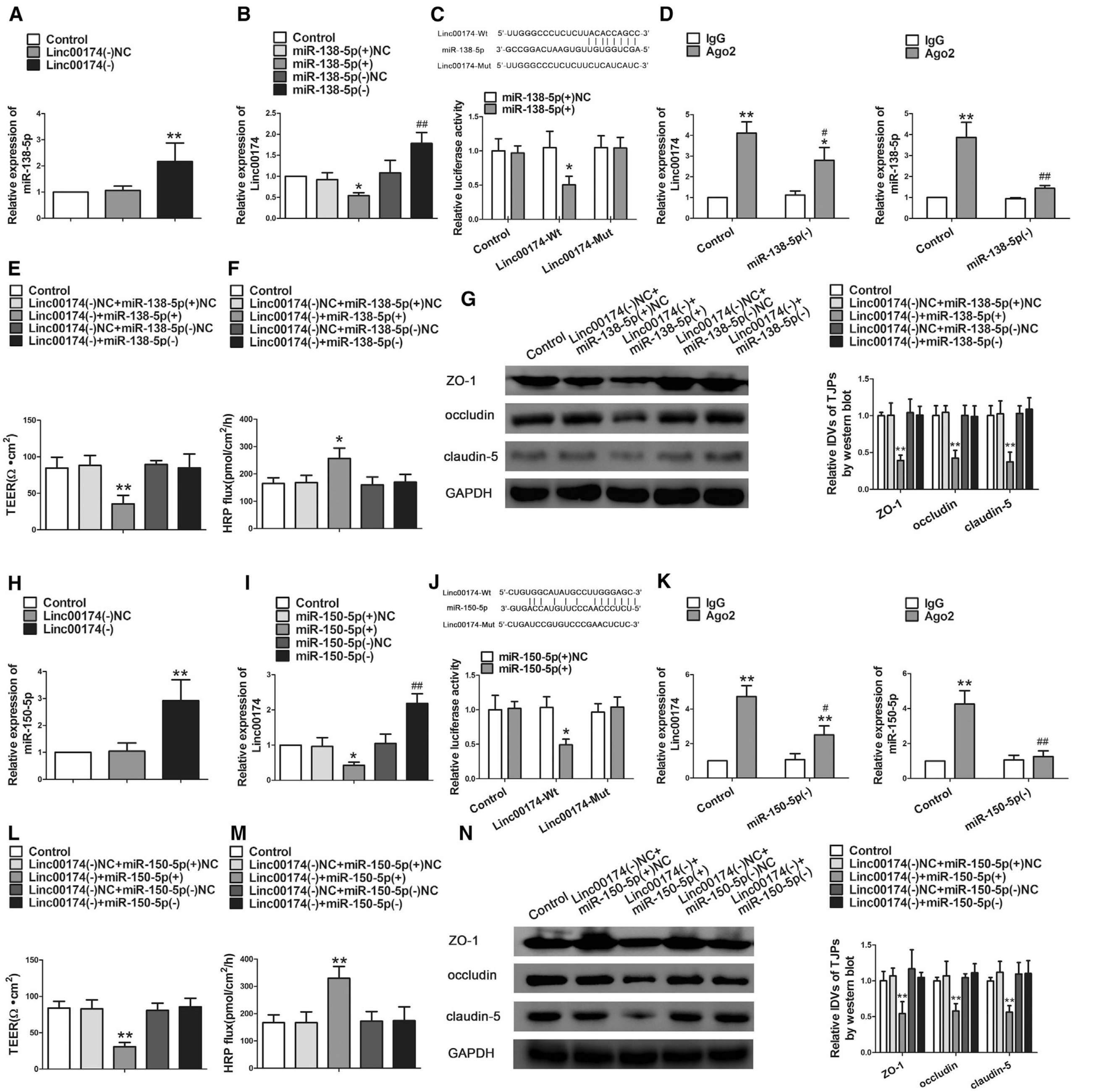

Figure 3. linc00174 Regulated BTB Permeability and the Expression of Tight Junction-Related Proteins by Binding to miR-138-5p and miR-150-5p in GECs
(A) Relative miR-138-5p expression was detected by quantitative real-time PCR after knock down of linc00174 in GECs. Data represent mean ± SD (n = 3, each). **p < 0.01 versus linc00174(−)NC group. (B) Relative linc00174 expression was detected by quantitative real-time PCR after changing miR-138-5p in GECs. Data represent mean ± SD (n = 3, each). *p < 0.05 versus miR-138-5p(+)NC group; ##p < 0.01 versus miR-138-5p(−)NC group. (C) Relative luciferase activity was detected by a Dual-Luciferase reporter assay. Data represent mean ± SD (n = 5, each). *p < 0.05 versus linc00174-Wt+ miR-138-5p(+)NC group. (D) RIP assay was performed with normal mouse IgG or anti-Ago2. Relative expression levels of linc00174 and miR-138-5p were determined by quantitative real-time PCR. Data represent mean ± SD (n = 3, each). *p < 0.05 and **p < 0.01 versus IgG group. (E) TEER assay evaluated the effect of linc00174 and miR-138-5p on BTB integrity. (F) HRP flux assay evaluated the effect of linc00174 and miR-138-5p on BTB permeability. Data represent mean ± SD (n = 5, each). *p < 0.05 and **p < 0.01 versus linc00174(−)NC+miR-138-5p(+)NC group. (G) Western blot assay evaluated the effect on ZO-1, occludin, and claudin-5. Data represent mean ± SD (n = 3, each). **p < 0.01 versus linc00174(−)NC+miR-138-5p(+)NC group. (H) Relative miR-150-5p expression was detected by quantitative real-time PCR after knock down of linc00174 in GECs. Data represent mean ± SD (n = 3, each). **p < 0.01 versus linc00174(−)NC group. (I) Relative linc00174 expression was detected by quantitative real-time PCR after changing miR-150-5p in GECs. Data represent mean ± SD (n = 5, each). *p < 0.05 versus miR-150-5p(+)NC group; ##p < 0.01 versus miR-150-5p(−)NC group. (J) Relative luciferase activity was performed by Dual-Luciferase reporter assay. Data represent

(legend continued on next page)

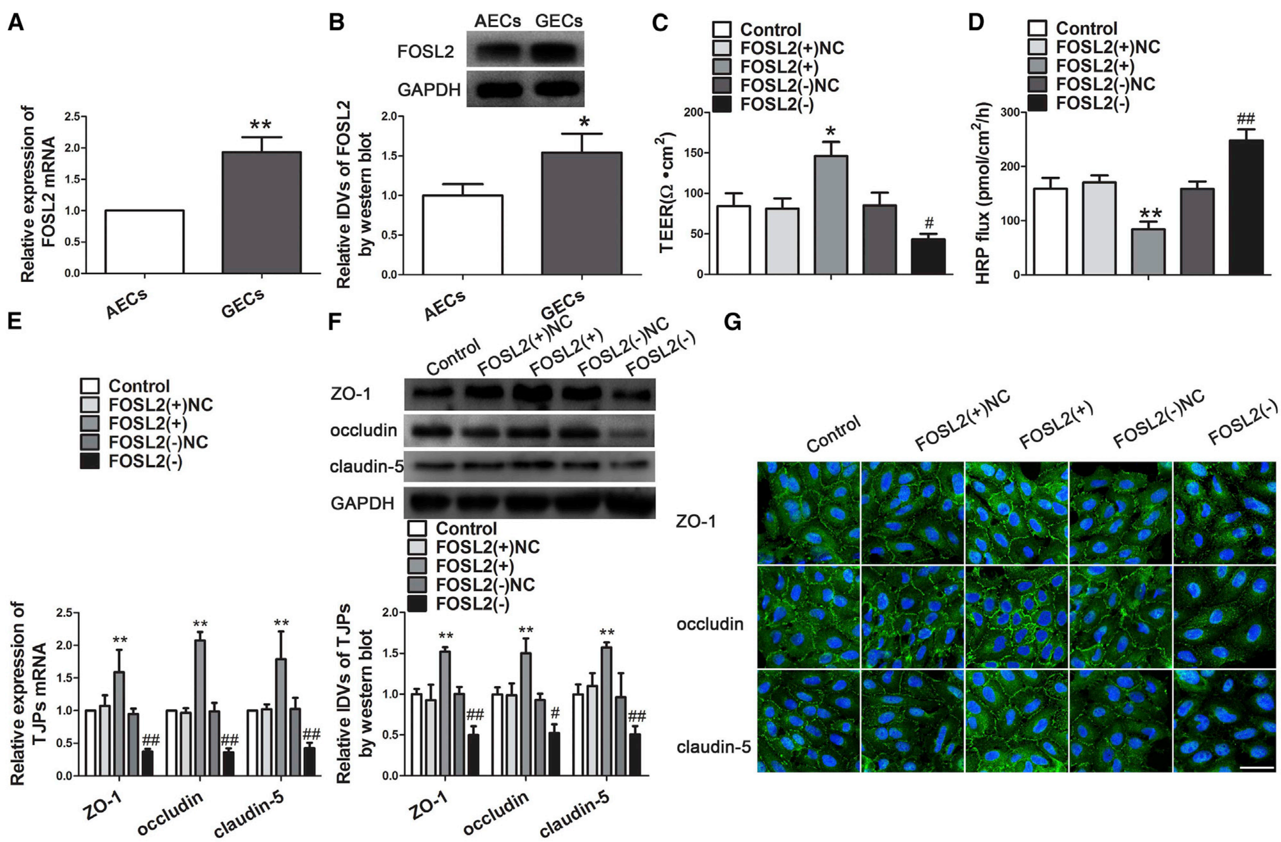

Figure 4. Knock Down of FOSL2 Increased BTB Permeability and Induced the Expression of Tight Junction-Related Proteins in GECs

(A) Relative expression levels of FOSL2 were detected by quantitative real-time PCR in AECs or GECs. $^{**}p < 0.01$ versus AECs group. (B) Western blot analysis of FOSL2 in AECs and GECs. Data represent mean ± SD (n = 3, each). $^{*}p < 0.05$ versus AECs group. (C) TEER assay evaluated the effect of FOSL2 on BTB integrity. (D) HRP flux assay evaluated the effect of FOSL2 on BTB permeability. Data represent mean ± SD (n = 5, each). $^{*}p < 0.05$ and $^{**}p < 0.01$ versus FOSL2(+)NC group; $^{\#}p < 0.05$ and $^{\#\#}p < 0.05$ versus FOSL2(−)NC group. (E) The mRNA expression of tight junction-related proteins was detected by quantitative real-time PCR. Data represent mean ± SD (n = 3, each). $^{**}p < 0.01$ versus FOSL2(+)NC group; $^{\#\#}p < 0.01$ versus FOSL2(−)NC group. (F) Western blot assay to evaluate the effect of FOSL2 on the protein expression of tight junction-related proteins in GECs. Data represent mean ± SD (n = 3, each). $^{**}p < 0.01$ versus FOSL2(+)NC group; $^{\#}p < 0.05$ and $^{\#\#}p < 0.01$ versus FOSL2(−)NC group. (G) Immunofluorescence location of tight junction-related protein in GECs after stable transfection of FOSL2(+), FOSL2(−), and FOSL2-NC. Images are representative of three independent experiments. Scale bar, 50 μm.

miR-138-5p or miR-150-5p overexpression decreased the mRNA and protein expression of FOSL2, whereas miR-138-5p or miR-150-5p inhibition exerted the opposite effects. Moreover, as shown in Figures 5G–5J, the mRNA and protein expressions of FOSL2 were significantly decreased in the linc00174(−)+miR-138-5p(+) group and linc00174(−)+miR-150-5p(+) group, compared with the linc00174(−)NC+miR-138-5p(+)NC group and linc00174(−)NC+miR-150-5p(+)NC group. However, miR-138-5p(+) and miR-150-5p(+) rescued the effects on FOSL2 expression decreased by linc00174(−). Furthermore, a luciferase assay was performed to detect whether FOSL2 was a direct target of miR-138-5p and miR-150-5p in GECs. As shown in Figures 5K and 5L, no significant difference was found in cells co-transfected with miR-138-5p(+) and FOSL2-3′ UTR-mutant (Mut) as well as in cells co-transfected with miR-150-5p(+) and FOSL2-3′ UTR-Mut. However, luciferase activity was significantly decreased in cells co-transfected with miR-138-5p(+) or miR-150-5p(+) and FOSL2-3′ UTR-Wt, compared with miR-138-5p(+)NC or miR-150-5p(+)NC and FOSL2-3′ UTR-Wt. The results suggested that FOSL2 was a directed target of both miR-138-5p and miR-150-5p.

mean ± SD (n = 3, each). $^{*}p < 0.05$ versus linc00174-Wt+miR-150-5p(+)NC group. (K) RIP assay was performed with normal mouse IgG or anti-Ago2. Relative expression levels of linc00174 and miR-150-5p were determined by quantitative real-time PCR. Data represent mean ± SD (n = 3, each). $^{*}p < 0.05$ and $^{**}p < 0.01$ versus IgG group. (L) TEER assay evaluated the effect of linc00174 and miR-150-5p on BTB integrity. (M) HRP flux assay evaluated the effect of linc00174 and miR-150-5p on BTB permeability. Data represent mean ± SD (n = 5, each). $^{**}p < 0.01$ versus linc00174(−)NC+miR-150-5p(+)NC group. (N) Western blot assay to evaluate the effect on ZO-1, occludin, and claudin-5. Data represent mean ± SD (n = 3, each). $^{**}p < 0.01$ versus linc00174(−)NC+miR-150-5p(+)NC group.

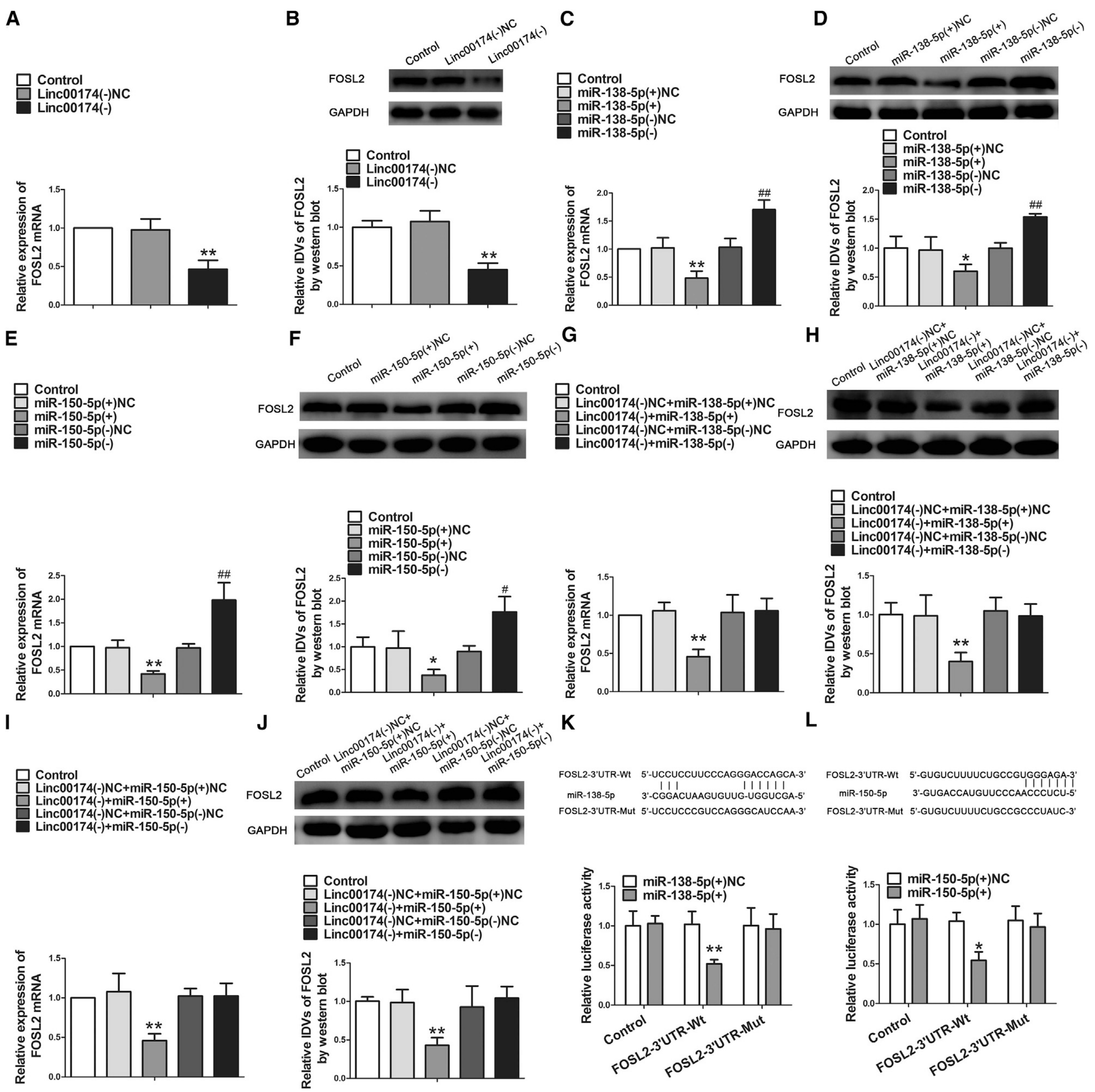

Figure 5. miR-138-5p/miR-150-5 Targeted FOSL2 3′ UTR

(A) Relative expression of FOSL2 mRNA was detected by quantitative real-time PCR in GECs after knock down of linc00174. (B) Relative IDVs of FOSL2 was detected by western blot in GECs with linc00174 inhibition. Data represent mean ± SD (n = 3, each). **p < 0.01 versus linc00174(−)NC group. (C) Relative expression of FOSL2 mRNA was detected by quantitative real-time PCR in GECs after changing miR-138-5p. (D) Relative IDVs of FOSL2 was detected by western blot in GECs after changing miR-138-5p. Data represent mean ± SD (n = 3, each). *p < 0.05 and **p < 0.01 versus miR-138-5p(+)NC group; ##p < 0.01 versus miR-138-5p(−)NC group. (E) Relative expression of FOSL2 mRNA was detected by quantitative real-time PCR in GECs after changing miR-150-5p. (F) Relative IDVs of FOSL2 was detected by western blot in GECs after changing miR-150-5p. Data represent mean ± SD (n = 3, each). *p < 0.05 and **p < 0.01 versus miR-150-5p(+)NC group; #p < 0.05 and ##p < 0.01 versus miR-150-5p(−)NC group. (G) linc00174 co-transfection with miR-138-5p. Relative expression of FOSL2 mRNA was detected by quantitative real-time PCR. (H) linc00174 co-transfection with miR-138-5p. Relative IDVs of FOSL2 was detected by western blot. Data represent mean ± SD (n = 3, each). **p < 0.01 versus linc00174(−)NC + miR-138-5p(+)NC group. (I) linc00174 co-transfection with miR-150-5p. Relative expression of FOSL2 mRNA was detected by quantitative real-time PCR. (J) linc00174 co-transfection with miR-150-5p. Relative IDVs of FOSL2 was detected by western blot. Data represent mean ± SD (n = 3, each). **p < 0.01 versus linc00174(−)NC + miR-150-5p(+)NC group. (K) Relative luciferase activity was detected by Dual-Luciferase assay. Data represent mean ± SD (n = 3, each). **p < 0.01 versus FOSL2-3′ UTR-Wt+miR-138-5p(+)NC group. (L) Relative luciferase activity was detected by Dual-Luciferase assay. Data represent mean ± SD (n = 5, each). *p < 0.05 versus FOSL2-3′ UTR-Wt+miR-150-5p(+)NC group.

FOSL2 Mediated the Tumor-Suppressive Effects of miR-138-5p and miR-150-5p in GECs

To clarify whether FOSL2 was involved in miR-138-5p or miR-150-5p overexpression in regulating BTB permeability, co-transfections between miR-138-5p or miR-150-5p and FOSL2 were conducted. Results showed that overexpression of FOSL2 with overexpression of miR-138-5p or miR-150-5p rescued the promotion effects on miR-138-5p or miR-150-5p overexpression on BTB permeability (Figures 6A, 6B, 6E, and 6F). Furthermore, FOSL2 overexpression largely rescued the effects on ZO-1, occludin, and claudin-5 downregulated by miR-138-5p or miR-150-5p overexpression (Figures 6C, 6D, 6G, and 6H). These results suggested that FOSL2 was involved in the effects of miR-138-5p or miR-150-5p overexpression on BTB permeability.

FOSL2 Upregulated Promoter Activities and Bound to the Promoters of ZO-1, Occludin, and Claudin-5

Knock down of FOSL2 reduced the expression of mRNA and protein of ZO-1, occludin, and claudin-5. In this study, to further verify whether FOSL2 regulated the promoters of ZO-1, occludin, and claudin-5 at the transcriptional level, luciferase assays and chromatin immunoprecipitation (ChIP) assays were conducted. The sequences of ZO-1, occludin, and claudin-5 promoters were set using Database: DBTSS. Positions of transcription start sites (TSSs) of ZO-1, occludin, and claudin-5 were predicted by DBTSS. Then, we analyzed these DNA sequences in the 2,000-bp region upstream of the TSS and its 100-bp downstream sequence. DNA fragments were constructed and ligated into the pGL3 basic vector. For co-transfection with pEX3-FOSL2, ZO-1 promoter activity was upregulated at −805 binding sites, but no significant difference was found with deletion of the −805 region. Similarly, occludin promoter activities were upregulated by the −824 region, but no significant difference was found with deletion of the −824 region and −206 region. Claudin-5 promoter activities were upregulated by the −798 binding site, but no significant difference was found with deletion of the −798 region and −698 region and −552 region (Figures 7A–7C).

Furthermore, a ChIP assay was performed to determine whether FOSL2 directly bound to the promoters of ZO-1, occludin, and claudin-5. The putative FOSL2 binding sites were indicated, and primers were designed. In addition, as for the NC, PCR was conducted to amplify the 1,000-bp upstream region that was not expected to associate the putative FOSL2. As shown in Figures 7D–7F, there were associations with FOSL2 binding sites PCR1 of ZO-1, PCR2 of occludin, and PCR3 of caludin-5, respectively. There was no association of FOSL2 with all of the control regions.

FOSL2 Feedback Promoted linc00174 Expression via Binding to Its Promoters

Database: JASPAR was used to identify the putative FOSL2 binding sites within the promoter region of linc00174. Figure 7G shows that linc00174 expression was significantly increased in the FOSL2(+) group, compared with the FOSL2(+)NC group. However, linc00174 expression was decreased in the FOSL2(−) group, compared with the FOSL2(−)NC group. Furthermore, a luciferase assay was conformed to clarify whether FOSL2 bound to the promoter of linc00174. The putative FOSL2 binding sites in linc00174 promoter were confirmed. Figure 7H shows that deletion of the region surrounding the −1886 site significantly increased linc00174 promoter activity. However, deletion of the region surrounding the −1716 site significantly reduced linc00174 promoter activity. In addition, no significant difference was found after deletion of the −579 site and deletion of the −31 site. Moreover, ChIP assays showed an interaction between FOSL2 and the linc00174 putative binding sites. Figure 7I shows the interaction with linc00174 binding sites at PCR3 of FOSL2, but no interaction with PCR1, PCR2, PCR4, and PCR5.

Knock Down of linc00174 Combined with miR-138-5p Overexpression or miR-150-5p Overexpression, and miR-138-5p Overexpression Combined with miR-150-5p Overexpression, Enhanced the Anti-tumor Effects of Doxorubicin

In this study, we co-transfected knock down of linc00174 and overexpression of miR-138-5p or miR-150-5p and co-transfected miR-138-5p or miR-150-5p overexpression separately. After the establishment of the BTB model, doxorubicin (Dox) (10 μM) was added and co-cultured for 12 h. We further performed flow cytometry to detect apoptosis of U87 cells in the lower chamber with annexin V-phycoerythrin (PE)/7-aminoactinomycin D (7AAD) double staining. As shown in Figure 8A, the apoptosis rate of U87 in the Dox group is significantly higher than that in the control group. Compared with the linc00174(−)+miR-138-5p(+) group, the apoptosis rate in the linc00174(−)+miR-138-5p(+)+Dox group was significantly increased. Similarly, the linc00174(−)+miR-150-5p(+)+Dox group showed the similar results. However, the apoptosis rate in the miR-138-5p(+)+miR-150-5p(+)+Dox group was higher than in the miR-138-5p(+)+miR-150-5p(+) group. Clearly, the rate of apoptosis in the linc00174(−)+miR-138-5p(+)+Dox group, the linc00174(−)+miR-150-5p(+)+Dox group, and the miR-138-5p(+)+miR-150-5p(+)+Dox group is higher than that in the Dox group. The schematic representation of the linc00174/miR-138-5p/miR-150-5P/FOSL2 feedback loop in BTB permeability was shown in Figure 8B.

DISCUSSION

In the present study, we have found that linc00174 was highly expressed in GECs. Knock down of linc00174 increased the BTB permeability and decreased the expression of tight junction proteins ZO-1, occludin, and claudin-5 by binding to miR-138-5p and miR-150-5p, which were downregulated in GECs. Meanwhile, downregulation of linc00174 inhibited FOSL2 expression. Furthermore, FOSL2 upregulated the promoter activities and bound to the promoter region of ZO-1, occludin, and claudin-5 in GECs. Moreover, FOSL2 regulated linc00174 expression by binding to its promoters, forming a positive feedback loop. In addition, combination of linc00174 knockdown and miR-138-5p overexpression or miR-150-5p overexpression and treated with Dox enhanced the anti-tumor effects of Dox.

The BTB consists of tight junctional proteins, which play a pivotal role in delivery of macromolecular anti-tumor drugs into tumor

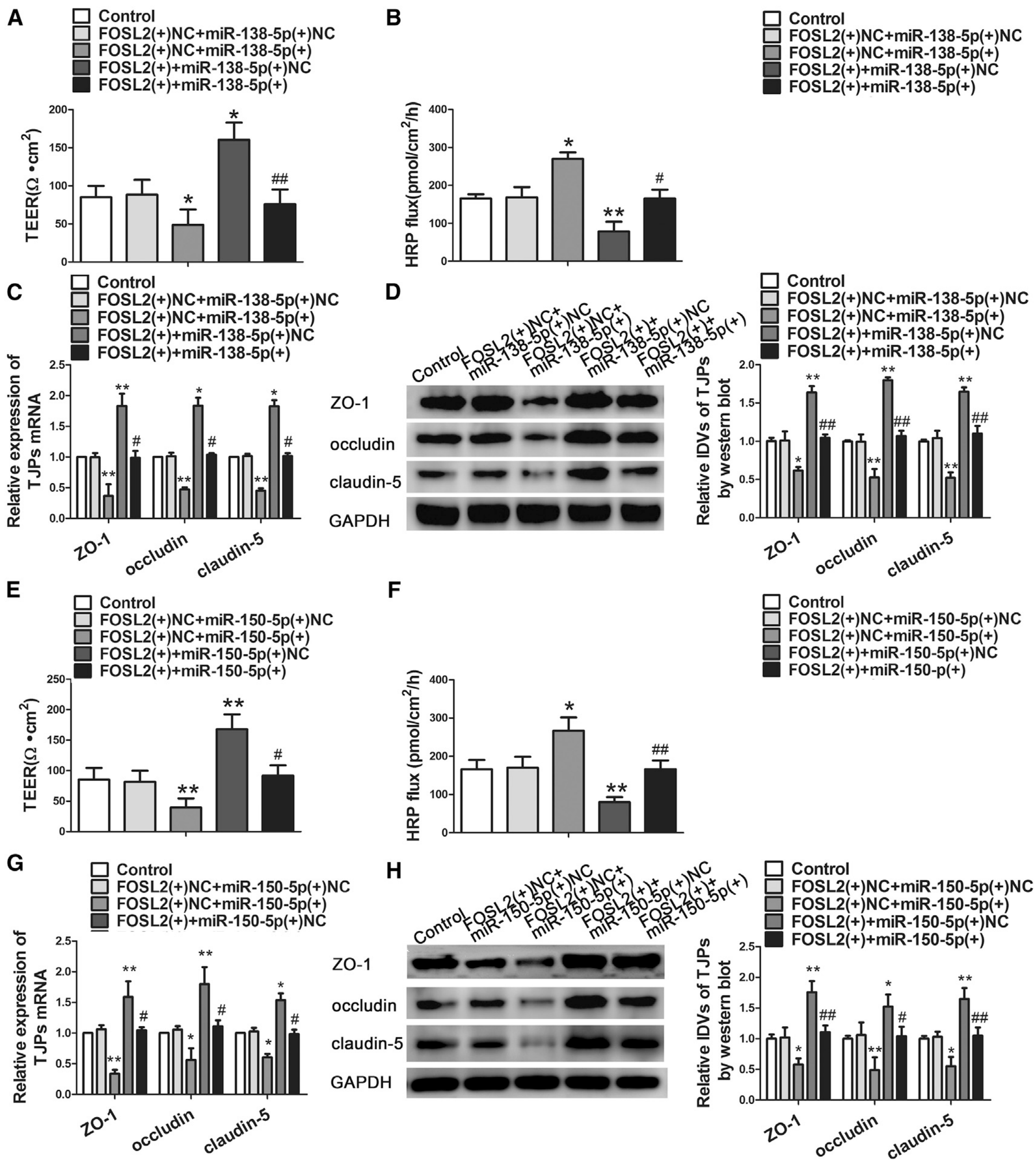

Figure 6. FOSL2 Mediated the Effects of miR-138-5p and miR-150-5p Overexpression on BTB Permeability in GECs

(A) TEER assay evaluated the effect of FOSL2 and miR-138-5p on BTB integrity. (B) HRP flux assay evaluated the effect of FOSL2 and miR-138-5p on BTB permeability. Data represent mean ± SD (n = 5, each). *p < 0.05 and **p < 0.01 versus FOSL2(+)NC+miR-138-5p(+)NC group; #p < 0.05 and ##p < 0.01 versus FOSL2(+)NC+miR-138-5p(+) group. (C) Relative expressions of tight junction-related proteins ZO-1, occludin, and claudin-5 mRNAs were detected by quantitative real-time PCR. (D) Relative IDVs of tight junction-related proteins were detected by western blot. Data represent mean ± SD (n = 3, each). *p < 0.05 and **p < 0.01 versus FOSL2(+)NC+miR-138-5p(+)NC group; #p < 0.05 versus FOSL2(+)NC+miR-138-5p(+)group. (E) TEER assay evaluated the effect of FOSL2 and miR-150-5p on BTB integrity. (F) HRP flux assay evaluated the effect of FOSL2 and miR-150-5p on BTB permeability. Data represent mean ± SD (n = 5, each). *p < 0.05 and **p < 0.01 versus FOSL2(+)NC+miR-150-5p(+)NC group; #p < 0.05 and ##p < 0.01 versus FOSL2(+)NC+miR-150-5p(+)group. (G) Relative expressions of tight junction-related proteins ZO-1, occludin, and claudin-5 mRNAs were detected by quantitative real-time PCR. (H) Relative IDVs of tight junction-related proteins were detected by western blot. Data represent mean ± SD (n = 3, each). *p < 0.05, and **p < 0.01 versus FOSL2(+)NC+miR-150-5p(+) NC group; #p < 0.05 versus FOSL2(+)NC+miR-150-5p(+)group.

tissues.[24,25] The BTB model was established with ECs and glioma cells *in vitro*. The TEER value and HRP flux were measured to reflect the integrity and permeability of the BTB, respectively. A recent study has showm that the expression of tight junctional protein ZO-1, occludin, and claudin-5 decreased when BTB permeability increased.[26]

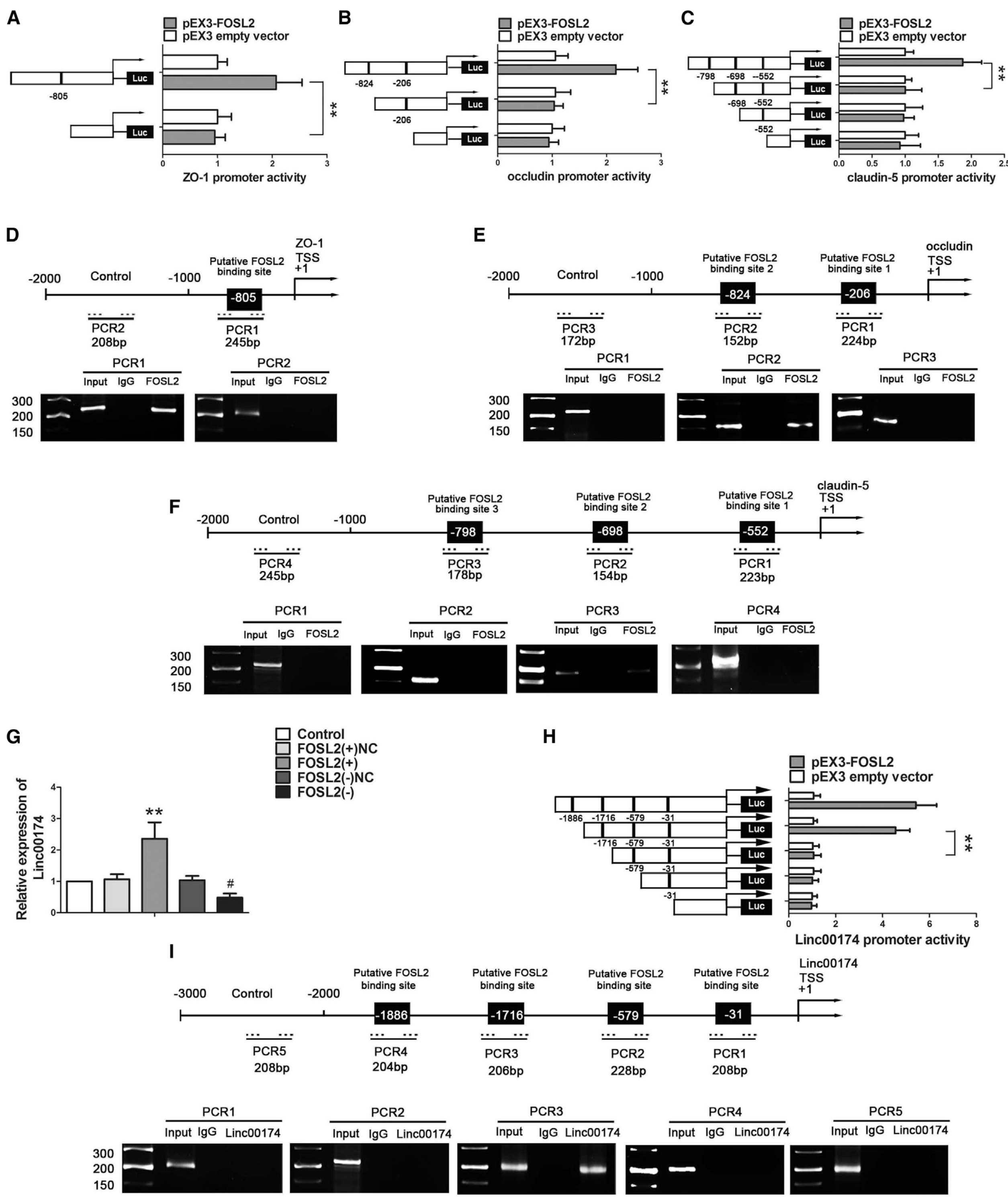

Figure 7. FOSL2 Bound to Promoters of ZO-1, Occludin, and Claudin-5 in GECs; Alternatively, FOSL2 Bound to the Promoter of linc00174 and Promoted Its Expression

(A and B) Schematic depictions of different reporter plasmids and relative luciferase activity in ZO-1 (A), occludin (B), and claudin-5 (C). The y axis shows the deletion positions on the promoter fragment. The x axis shows the reporter vector activity after co-transfection of the reference vector (pRL-TK) and relative to the activity of the pEX3 empty vector, the activity of which was set to 1. Schematic representation of the human ZO-1, occludin, and claudin-5 promoter regions 2,000 bp upstream of the transcription start

(legend continued on next page)

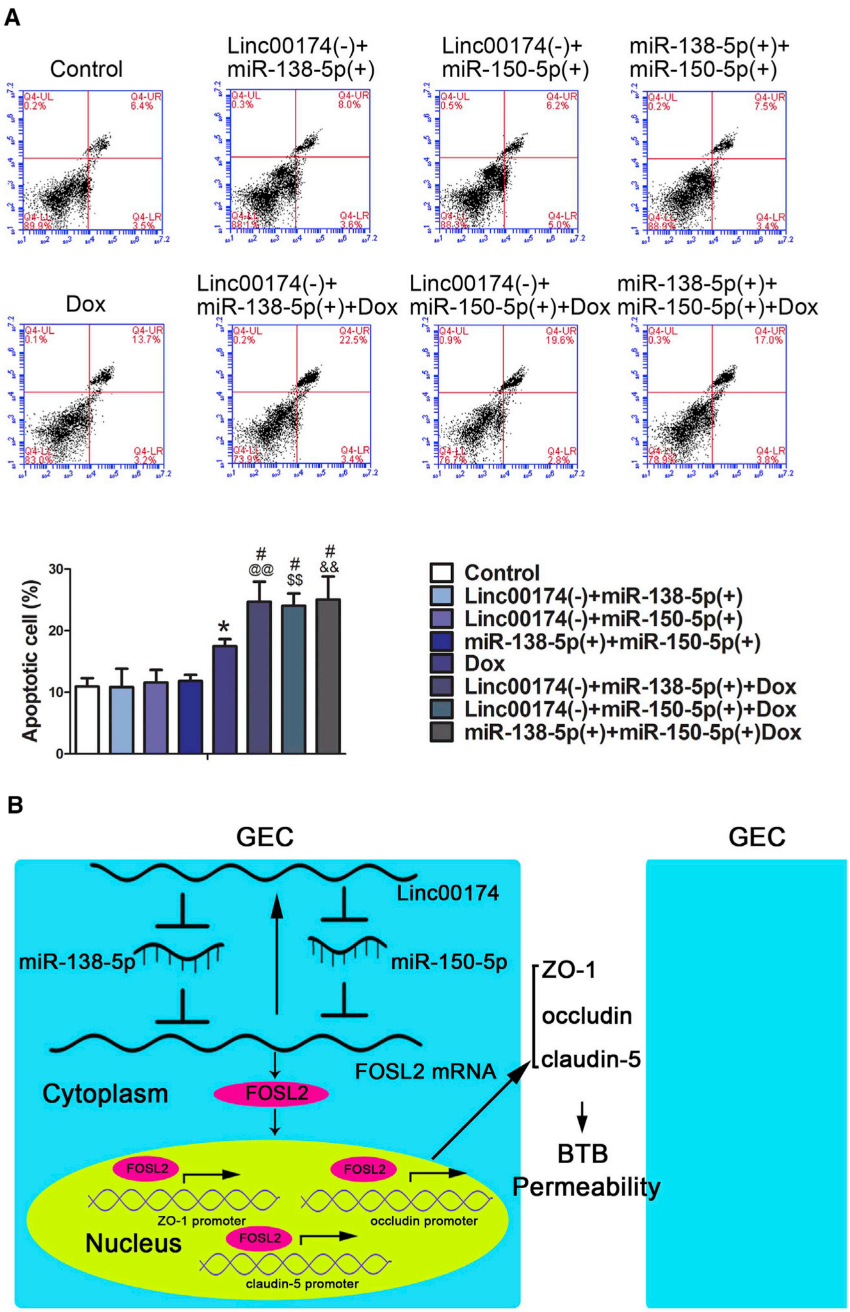

Figure 8. linc00174 Combined with miR-138-5p or miR-150-5p Enhanced the Anti-tumor Effect of Dox; Alternatively, It Further Enhanced the Feedback Loop

(A) The apoptosis of U87 cells was significantly increased by co-transfection of linc00174 and miR-138-5p or miR-150-5p treated with doxorubicin (Dox) (10 μM). Data represent mean ± SD (n = 3, each). $^{*}p < 0.05$ versus control group; $^{\#}p < 0.05$ versus Dox group; $^{@@}p < 0.01$ versus linc00174(−)+miR-138-5p(+) group; $^{\$\$}p < 0.01$ versus linc00174(−)+miR-150-5p(+) group; $^{\&\&}p < 0.01$ versus miR-138-5p(+) +miR-150-5p(+) group. (B) Cartoon of the mechanisms of the linc00174/miR-138-5p/miR-150-5p/FOSL2 feedback loop regulating permeability of BTB.

Emerging evidence shows that non-coding RNAs are not only involved in regulating tumor development, but they regulate BTB permeability as well. MEG3 overexpression increased BTB permeability by inhibiting the expression of miR-330-5p in GECs.[27] Knock down of SNHG12 expression reduces viability and mobility, meanwhile increasing apoptosis of human glioma cells.[28] In addition, MALAT1,[29] XIST,[30] and miR-429[31] have been demonstrated to participate in regulating the BTB permeability. linc00174, a lncRNA with the length of 4,462 bp, is found to be expressed in normal brain tissue and to have high expression in testicular tissue using Database: NONCODE. In addition, a recent study has shown that linc00174 promotes the progression of colorectal cancer by combining with miR-1910-3p.[32] Furthermore, in this study, we found that linc00174 was upregulated in GECs. Knock down of linc00174 increased the permeability of the BTB by downregulating the expression of tight junction proteins ZO-1, occludin, and claudin-5, indicating that linc00174 inhibition increased the permeability of the BTB through the paracellular pathway.

Recent studies have shown that miRNAs are involved in the regulation of endothelial cell function. Overexpression of miR-18a decreases the expression of tight junction proteins ZO-1 occludin and claudin-5 through RUNX1.[33] miR-34a regulates the function of the BTB by targeting protein kinase C (PKC)ε.[34] miR-138-5p is involved in the regulation of the pathological process of many diseases. miR-138-5p shows low expression in osteoarthritis,[35] and it acts as a tumor suppressor in bladder cancer.[36] Moreover, in retinoblastoma, overexpression of miR-138-5p decreased the

site (TSS, designated as +1) are shown. Chromatin immunoprecipitation (ChIP) PCR products for putative FOSL2 binding sites and an upstream region not expected to associate with FOSL2 were amplified by PCR using their specific primers. (D–F) PCR of ZO-1 (D), occludin (E), and claudin-5 (F) was conducted with the resulting precipitated DNA. Image is representative of independent ChIP experiments. (G) Relative expression of linc00174 after stabilized transection with FOSL2. Data represent mean ± SD (n = 3, each). $^{**}p < 0.01$ versus FOSL2(+)NC group; $^{\#}p < 0.05$ versus FOSL2(−)NC group. (H) Schematic depiction of different reporter plasmids and relative luciferase activity in linc00174. Schematic representation of the human linc00174 promoter region is shown. (I) ChIP PCR products for putative FOSL2 binding sites and an upstream region not expected to associate with FOSL2 were amplified by PCR using their specific primers. PCR of linc00174 was conducted with the resulting precipitated DNA.

expression of pyruvate dehydrogenase kinase 1 (PDK1), repressed retinoblastoma cell viability, migration, and invasion, and induced apoptosis of retinoblastoma cells.[37] In addition, miR-150-5p is downregulated in circulating blood of patients with delayed myasthenia gravis and acts as a biomarker.[38] miR-150-5p is downregulated in head and neck squamous carcinoma cells.[39] Overexpression of miR-150-5p inhibits the proliferation, migration, invasion, and epithelial interstitial transformation of non-small cell lung cancer cells.[13] In this study, we found that miR-138-5p and miR-150-5p were downregulated in GECs. Overexpressing miR-138-5p or miR-150-5p, respectively, increased BTB permeability and decreased the expression and distribution of ZO-1, occludin, and claudin-5.

Several recent studies have confirmed that lncRNAs regulate the expression of miRNAs and act as a competing endogenous RNA (ceRNA) or a molecular sponge.[40,41] MEG3 regulates BTB permeability through direct binding to miR-330-5p and negatively regulating its expression.[27] linc00174 acts as ceRNA to promote the progression of colorectal cancer through binding to miR-1910-3p.[32] In our study, knock down of linc00174 increased the expression of miR-138-5p and miR-150-5p. Furthermore, bioinformatics analysis (starBase v2.0) and a luciferase reporter assay were used to find miR-138-5p and miR-150-5p direct binding, respectively, to linc00174. Moreover, upregulation of miR-138-5p or miR-150-5p suppressed the linc00174 expression; however, downregulating miR-138-5p or miR-150-5p showed the opposite results, which indicated that there was a reciprocal repression between linc00174 and miR-138-5p or miR-150-5p. Furthermore, a RIP assay was conducted to explore the underlying mechanism of lncRNA and miRNA regulatory function. Similar to our results, studies support the reciprocal repression process induced by the RNA silencing complex. lncRNA FTH1P3 sponging to miR-206 regulates ABCB1 expression in breast cancer.[42] SNHG7 is upregulated in lung cancer and functioned as ceRNA-antagonized miR-193b upregulating the FAIM2 expression level to inhibit cell proliferation and metastasis.[43] FOSL2 plays an important role in regulating biological functions of cancer.[44] The expression of FOSL2 is remarkably increased in the skin tissue of systemic sclerosis (SSc) animal models, which is likely to be directly involved in the activation of SSc fibroblasts.[45] Moreover, FOSL2 is abundantly detected in ECs and vascular smooth muscle cells of SSc lesional skin, and silencing FOSL2 promotes angiogenesis in human microvascular ECs.[46,47] In this study, we found that FOSL2 was upregulated in GECs. Knock down of FOSL2 increased BTB permeability and decreased the expression of ZO-1, occludin, and claudin-5.

Accumulating studies showed that miRNAs negatively regulate target gene expression through binding to the 3′ UTR of target mRNA.[48] In non-small cell lung cancer, miR-550a-3p represses the expression of TIMP2 via binding to the TIMP2 3′ UTR, whereas it promotes the growth and metastasis of non-small cell lung cancer cells.[49] miR-200a reduces PTEN expression by binding to the PTEN 3′ UTR, and it significantly enhances the migratory and invasive abilities of ovarian carcinoma cells.[50] The results of bioinformatics analysis and luciferase assays indicated that FOSL2 was one of the direct targets of miR-138-5p and miR-150-5p in regulating the permeability of the BTB. Furthermore, overexpression of FOSL2, which stably overexpresses miR-138-5p or miR-150-5p, largely rescued the regulation of miR-138-5p and miR-150-5p on BTB permeability through downregulating the expression of ZO-1, occludin, and claudin-5. Similar to our results, miR-140 shows downregulation, and transcription factor NFYA is upregulated in GECs. Restored expression of miR-140 significantly decrease the expression of ZO-1, occludin, and claudin-5 and increases BTB permeability through negatively regulating NFYA.[29] Moreover, miR-18a overexpression decreases the expression of ZO-1, occludin, and claudin-5 and increases BTB permeability by negative regulation of MEF2D and KLF4 in GECs.[51] The mechanism by which miRNAs regulate BTB permeability has increasingly attracted the attention.

Furthermore, in this study, to elucidate whether FOSL2 interacted with the promoters of ZO-1, occludin, and claudin-5, luciferase reporter and ChIP assays were performed. The results showed that FOSL2 directly bound to the promoter region of tight junction proteins ZO-1, occludin, and claudin-5 and upregulated promoter activities. A recent study shows that FOSL2 transactivates TIMP-1 by directly binding to the promoter of TIMP-1 while promoting fibrogenesis in mice.[52] Knock down of FOSL2 in human adipocytes decreased leptin (LEP) expression at the transcriptional level, reducing adiposity.[53] Also, signal transducer and activator of transcription 5 (STAT5) activates and binds to the promoter of FOSL2, regulating key immunological processes in CD4 T cells.[54] In addition, an ongoing study has indicated that lncRNAs can be regulated by transcription factors. Nuclear factor κB (NF-kB) binds to the lncRNA NEAT1 promoter to activate NEAT1 expression and promotes lung cancer cell proliferation and migration.[55] lncRNA ERIC is regulated by E2F and modulates the cellular response to DNA damage.[56] In this study, we demonstrated that FOSL2 directly bound to the promoter region of linc00174 and upregulated promoter activities. Overexpression of FOSL2 significantly increased linc00174 expression. However, inhibition of FOSL2 decreased linc00174 expression. The results indicated that the linc00174/miR-138-5p/miR-150-5p/FOSL2 axis regulated BTB permeability by forming a positive feedback loop. Recent study shows that transfection factor FOXO1 binds to MALAT1 promoter region and negatively regulates MALAT1 expression. The FOXO1/MALAT1/miR-26a-5p feedback loop mediates proliferation and migration in osteosarcoma cells.[57] lncRNA HCP5 promotes glioma cell progression through regulating RUNX1 expression. Meanwhile, the transcription factor RUNX1 binds to the promoter of HCP5 and promotes HCP5 expression.[58] Furthermore, the GAS5/miR-196a-5p/FOXO1 feedback loop suppresses malignancy of human glioma stem cells.[59]

Remarkably, we finally demonstrated that knock down of linc00174 combined with overexpression of miR-138-5p or miR-150-5p, which when treated with Dox significantly increased glioma cell apoptosis. This study demonstrated that the combination of silencing

Table 1. Primers and Probes Used for Quantitative Real-Time PCR

Primer or Probe	Gene	Sequence (5′ → 3′) or Assay ID
Primer	linc00174	F: TGTGTCTACAGGCCCAACTG
		R: AAGGTGGGCCTAGCAAAGTT
	FOSL2	F: GGGTAGATATGCCTGGCTCA
		R: GGTATGGGTTGGACATGGAG
	GAPDH	F: AAATCCCATCACCATCTTCCAG
		R: TGATGACCCTTTTGGCTCCC
Probe	miR-138-5p	2452336 (Applied Biosystems)
	miR-150-5p	2824926 (Applied Biosystems)
	U6	2819045 (Applied Biosystems)

One-Step SYBR PrimeScript RT-PCR cycling conditions were as follows: 5 min at 42°C, 10 s at 95°C, 40 cycles of 3 s at 95°C, and 30 s at 60°C. The reverse transcription was set as follows: 30 min at 16°C, 30 min at 42°C, and 5 min at 85°C. PCR conditions were set as follows: 2 min at 50°C, 10 min at 95°C, 40 cycles of 15 s at 95°C, and 1 min at 60°C. F, forward; R, reverse.

linc00174 and overexpression of miR-138-5p or miR-150-5p could enhance the anti-tumor effects of Dox in the *in vitro* BTB model.

In conclusion, this study demonstrated that the expression of linc00174 and FOSL2 were upregulated while the expression of miR-138-5p and miR-150-5p were downregulated in GECs for the first time. Knock down of linc00174 increased BTB permeability by upregulating miR-138-5p and miR-150-5p through FOSL2 inhibition. Moreover, FOSL2 inhibition enhanced BTB permeability by transcriptional repression of ZO-1, occludin, and claudin-5. These findings may contribute to develop effective strategies for treating glioma.

MATERIALS AND METHODS

Cell Line and Culture

An immortalized human cerebral microvascular endothelial cell line (hCMEC/D3; ECs) was presented by Dr. P.-O. Couraud (Institut Cochin, Paris, France). ECs were limited from 30 to 35 passages in this present study. ECs were cultured on culture chambers covered with 150 μg/mL Cultrex rat collagen I (R&D Systems, Minneapolis, MN, USA) and in endothelial basal medium (EBM-2; Lonza, Walkersville, MD, USA) with 5% fetal bovine serum (FBS) Gold (PAA Laboratories, Pasching, Austria), 1% penicillin-streptomycin (Life Technologies, Paisley, UK), 1.4 μM hydrocortisone (Sigma-Aldrich, St. Louis, MO, USA), 1% chemically defined lipid concentrate (Life Technologies, Paisley, UK), 5 μg/mL ascorbic acid (Sigma-Aldrich, St. Louis, MO, USA), 10 mM HEPES (PAA Laboratories, Pasching, Austria), and 1 ng/mL human basic fibroblast growth factor (bFGF; Sigma-Aldrich, St. Louis, MO, USA).

The human glioma cell line U87MG, normal human astrocytes, and the HEK293T cell line were purchased from the Shanghai Institutes for Biological Sciences Cell Resource Center. Cells were cultured in DMEM, which contains high-glucose-containing 10% FBS, 100 U/mL penicillin, and 100 μg/mL streptomycin (Life Technologies, Paisley, UK). All cells were maintained in a humidified incubator (37°C, 5% CO_2). Normal brain tissues and four grade of human brain tissues obtained from patients who have signed the Informed consent hospitalized in the Department of Neurosurgery of Shengjing Hospital of China Medical University, moreover our study was approved by the Ethics Committee of Shengjing Hospital of China Medical University.

Establishment of a BTB Model *In Vitro*

We established an *in vitro* BTB model by co-culturing ECs with normal human astrocytes and U87 glioma cells in a Transwell permeable support system as described previously.[26] In brief, U87 cells were seeded at 2×10^4 per well in six-well plates with suitable culture medium and cultured for 2 days. ECs were seeded at 2×10^5 per well on the upper side of chambers pre-covered freshly with 150 μg/mL Cultrex rat collagen I (R&D Systems, Minneapolis, MN, USA). The system was cultured with prepared EBM-2 medium, and then the medium was renewed every 2 days. After co-culturing 4 days, GECs and AECs were obtained and used for the next study.

Quantitative Real-Time PCR Assay

The expression levels of linc00174, miR-138-5p, miR-150-5p, and FOSL2 were determined by quantitative real-time PCR. Total RNA was separated from the cultured cells with TRIzol reagent (Life Technologies, Carlsbad, CA, USA), following the manufacturer's instructions. The RNA concentration and quality were determined in each sample by the 260/280 nm ratio using a NanoDrop 2000 spectrophotometer (ND-100, Thermo Scientific, USA). To measure linc00174 and FOSL2 expression, quantitative real-time PCR was performed using a SYBR PrimeScript RT-PCR kit (Takara Bio). For quantification of miR-138-5p and miR-150-5p expression, reverse transcription was first carried out with TaqMan Micro RNA reverse transcription kits (Applied Biosystems, Foster City, CA, USA), according to the manufacturer's protocol. Then, TaqMan Universal Master Mix II (Applied Biosystems) was used to detect the probes for miR-138-5p (2452336), miR-150-5p (2824926), and endogenous control U6 (2819045). All quantitative RT-PCR analyses were conducted by method of the 7500 Fast Real-Time PCR System (Applied Biosystems, Foster City, CA, USA). Relative expression values were calculated using the relative quantification ($2^{-\Delta\Delta Ct}$) method. These primers and probes used in this study listed in Table 1.

Cell Transfection

The short hairpin RNA (shRNA) directed against the human linc00174 gene or the FOSL2 gene was reconstructed in a pGPU6/GFP/Neo vector (linc00174(−) and FOSL2(−), respectively; Gene Pharma, Shanghai, China). Its empty vector was used as a NC (linc00174(−)NC, FOSL2(−)NC). The human FOSL2 gene-coding sequence was ligated into a pIRES2-EGFP vector (FOSL2(+)) (GenScript, Piscataway, NJ, USA), and its empty vector was used as a NC (FOSL2(+)NC). AECs were seeded in 24-well plates and transfected using LTX and Plus reagent (Life Technologies) when the confluence reached 70% to ~80%. Stable cell lines were selected

Table 2. Sequences of shRNA Template

Gene		Sequence (5′→3′)
linc00174	sense	CACCGCCCACAATGTACTCAGATCATCATTCAAGAGATGATCTGAGTACATTGTGGGCTTTTTTG
linc00174	antisense	GATCCAAAAAAGCCCACAATGTACTCAGATCATCTCTTGAATGATCTGAGTACATTGTGGGC
FOSL2	sense	CACCGCAGGAGGAGGAGAGATGAGCAGCTTCAAGAGAGCTGCTCATCTCTCCTCCTGCTTTTTTG
FOSL2	antisense	GATCCAAAAAAGCAGGAGGAGAGATGAGCAGCTCTCTTGAAGCTGCTCATCTCTCCTCCTGC
NC	sense	CACCGTTCTCCGAACGTGTCACGTCAAGAGATTACGTGACACGTTCGGAGAATTTTTTG
NC	antisense	GATCCAAAAAAGTTCTCCGAACGTGTCACGTAATCTCTTGACGTGACACGTTCGGAGAAC

through the medium containing Geneticin (G418; Sigma-Aldrich, St. Louis, MO, USA), and G418-resistant clones were obtained after 4 weeks. Agomir-138-5p (miR-138-5p(+)), antagomir-138-5p (miR-138-5p(−)), and their NC sequences (miR-138-5p(+)NC and miR-138-5p(−)NC; Gene Pharma) were transiently transfected into AECs, which stably transfected linc00174 inhibition or FOSL2 overexpression, respectively, according to the manufacturer's instructions using Lipofectamine 3000 reagent. Cells were collected 2 days after transfection. Sequences of linc00174(−), FOSL2(−), and NC are shown in Table 2. The transfection efficiency of linc00174, FOSL2, and miR-138-5p or miR-150-5p are shown in Figure S1.

TEER Assays

To measure the integrity and permeability of the BTB, a TEER assay was performed after *in vitro* BTB models were established with Millicell-ERS apparatus (Millipore, Billerica, MA, USA). In order to ensure temperature equilibration and uniformity of the culture environment, TEER was recorded after 30 min at room temperature and the culture medium was refreshed before each measurement. The final resistance ($\Omega \cdot cm^2$) was calculated by subtracting background resistance from measured barrier resistance, and multiplied by the effective surface area of the chamber membrane.

HRP Flux Assays

HRP flux assays were performed to measure BTB permeability. After BTB models were established, 1 mL of culture medium containing 10 μg/mL HRP (0.5 μM, Sigma-Aldrich, USA) was added into the upper compartment of the Transwell system, and 2 mL of culture medium was added to the well. One hour later, the 5 μL of culture medium in the lower chamber was collected from each well and the HRP content of the samples was assayed using tetramethylbenzidine (TMB) colorimetrically with a spectrophotometer at 370 nm. The final HRP permeability was calculated from the standard curve and expressed as picomoles passed per square centimeter of surface area per hour (pmol/cm^2/h).

Western Blot Assays

We used western blot analysis to detect protein expression levels of FOSL2 and tight junction-related proteins in *in vitro* BTB models. Cells were harvested and lysed in Radio Immunoprecipitation Assay (RIPA) Lysis Buffer (Beyotime Institute of Biotechnology, Jiangsu, China) mixed with PMSF (protease inhibitors) and centrifuged at 14,000 × *g* for 10 min at 4°C. After that, the protein concentration of the sample was measured with a bicinchoninic acid (BCA) protein assay kit (Beyotime Institute of Biotechnology, Jiangsu, China). Using SDS-PAGE, equal amounts of protein (40 μg) were separated and then transferred onto polyvinylidene fluoride (PVDF) membranes (Millipore, USA). After fulfilling with the blocking buffer (5% nonfat-dried Milk) for 2 h at room temperature, the membranes were incubated with primary antibodies against FOSL2 (1:500; Abcam, USA), glyceraldehyde-3-phosphate dehydrogenase (GAPDH; 1:10,000; Proteintech, Chicago, IL, USA), ZO-1 (1:300; Life Technologies, Frederick, MD, USA), occludin (1:600; Proteintech, Chicago, IL, USA), and claudin-5 (1:250; Proteintech, Chicago, IL, USA) at 4°C overnight. After washing the membranes with TTBS three times, they were incubated with the corresponding HRP-conjugated secondary antibody diluted at 1:10,000 at room temperature for 2 h. After three washes with TBST, followed by use of an enhanced chemiluminescence (ECL) kit (Beyotime Institute of Biotechnology, Jiangsu, China), visualized protein bands were detected with an ECL detection system (Thermo Scientific, USA). The protein bands were scanned using ChemiImager 5500 v2.03 software, and integrated light density values (IDVs) were calculated by Fluor Chen 2.0 software and normalized with GAPDH.

Immunofluorescence Assays

An immunofluorescence assay was performed to detect the expression and distribution of tight junction-related proteins in GECs. The cells should be 100% confluent when mixed with 4% paraformaldehyde for 30 min and permeated with 0.3% Triton X-100 for 10 min at room temperature (ZO-1, occludin, and claudin-5), or fixed with methanol for 10 min at −20°C (for occludin), followed by incubation in 5% BSA blocking buffer for 2 h at room temperature. Subsequently, cells were then incubated with primary antibodies for ZO-1 (1:50; Life Technologies, Frederick, MD, USA), occludin (1:50; Abcam, USA), and claudin-5 (1:50; Life Technologies, Frederick, MD, USA) overnight at 4°C. After three washes with PBST, cells were incubated with Alexa Fluor 555-labeled goat anti-mouse IgG or anti-rabbit IgG secondary antibody (1:500; Beyotime Institute of Biotechnology, Jiangsu, China) for 2 h. After washing with PBS with Tween 20 (PBST) three times, the nuclei were then stained with 0.5 μg/mL DAPI for 8 min. The staining was analyzed using immunofluorescence microscopy (Olympus, Tokyo, Japan) and merged by the ChemiImager 5500 v2.03 software.

Table 3. Primers Used for ChIP Experiments

Gene	Binding Site or Control	Sequence (5′→3′)	Product Size (bp)	Annealing Temperature (°C)
ZO-1	PCR1	F: CCGTCAACATTGTGGGAAG	245	55
		R: CCACACCCCACATTAGACCT		
	PCR2	F: GACACCAAAAATCCCACAGG	208	56.4
		R: CACACGCATGTCATCATAGC		
Occludin	PCR1	F: ACCCATTAAAGCTGCCATCA	152	55
		R: TCTATCCAATCCCACCCACT		
	PCR2	F: CTCAGGCCCAAGAGCCATAA	224	54.9
		R: TGTGTAAACATTGGCGCTGT		
	PCR3	F: ATGTTGGATTTGGGAAGCAG	172	56
		R: TGGAGCATTCACCAAGACAG		
Claudin-5	PCR1	F: CAGGTCCCTGATGACCTGAG	178	55
		R: TGGACATCTCCTCCTCTGTG		
	PCR2	F: TGTAGAGGAAGGGGCATGG	154	56.8
	PCR3	R: TGAGGCTGGAAGGAAATCAT	223	58
	PCR4	F: GGCTAAGCAAAGAGGGTATG	245	58.3
		R: AGGGCCCTCCATAGAAAAAG		
		F: TGAGGTTGGATGAGCTGTGA		
		R: GCGGGCATTGTTGTTACTCT		
FOSL2	PCR1	F: AAGGGTCCCGGGAGATAGAC	208	58.7
		R: CTCACCCCCAGCAGACAAAA		
	PCR2	F: GTGGGGGAGTCTTTTCCTTGA	228	57.4
		R: GGCACACACCTATAGTCCTACG		
	PCR3	F: GGAGGTTGAGGCAAGGAGAA	206	58
		R: CCACATACATTACTGGTGGGA		
	PCR4	F: TGGGCAAGATAGCAAGACCC	204	57.8
		R: TTGCCTCAACCTCCCGAGTA		
	PCR5	F: TGTAGATTCAAACTCCTGGGCT	208	56.5
		R: GCCTATAATCCCAGCACTTTGG		

Reporter Vector Construction and Luciferase Reporter Assay

The potential binding sequence of miR-138-5p and miR-150-5p in the linc00174 gene and its mutant sequence was amplified by PCR, synthesized, and cloned into the pmirGLO Dual-Luciferase vector (Promega, Madison, WI, USA). Wild-type pmirGLO-linc00174 (or linc00174 mutant) reporter plasmid and agomir-138-5p or agomir-138-5p-NC/agomir-150-5p or agomir-150-5p-NC were co-transfected into HEK293T cells. Luciferase activity was measured 2 days after transfection through the Dual-Luciferase reporter system (Promega). The 3′ UTR of FOSL2 containing the presumed miR-138-5p and miR-150-5p binding sequences and their mutant sequence were cloned into Dual-Luciferase vectors. Following the transfection approach, measurements of luciferase activities were performed as described above.

RNA Immunoprecipitation Assay

A Magna RNA-binding protein immunoprecipitation kit (Millipore) was used to perform RNA immunoprecipitation assays. Briefly, cells were lysed in complete RNA lysis buffer and cell lysates were incubated with human anti-Ago2 antibody (Millipore) and NC mouse IgG (Millipore). Samples were incubated with proteinase K buffer, and then immunoprecipitated RNA was isolated. Purified RNA was obtained and then applied to qPCR with reverse transcription analysis. A ChIP assay was performed using the SimpleChIP Enzymatic Chromatin IP kit (Cell Signaling Technology, Danvers, MA, USA) according to the manufacturer's instructions. Briefly, cells were cross-linked with EBM-2 containing 1% formaldehyde for 10 min, and glycine was added for 5 min at room temperature to quench the cross-link. Then, cells were collected in lysis buffer containing 1% PMSF. Chromatin was digested by micrococcal nuclease. Lysate (2%) was used as an input reference. Immunoprecipitation was incubated with 3 μg of anti-FOSL2 antibody (Abcam) or normal rabbit IgG followed by immunoprecipitation with protein G-agarose beads during an overnight incubation at 4°C with gentle shaking. The DNA cross-link was reversed by 5 M NaCl and proteinase K at 65°C for 2 h and then DNA was purified.

ChIP Assay

ChIP assays were performed with a SimpleChIP Enzymatic Chromatin IP kit (Cell Signaling Technology, Danvers, MA, USA) according to the manufacturer's protocol. Briefly, cells were cross-linked with 1% formaldehyde in culture medium for 10 min, and then glycine was added for 5 min at room temperature. These cells were collected in lysis buffer containing PMSF. Then, chromatin was digested by micrococcal nuclease and incubated for 20 min at 37°C with frequent mixing. Immunoprecipitation was incubated with 3 μg of anti-FOSL2 antibody followed by immunoprecipitation with protein G-agarose beads in each sample during an overnight incubation at 4°C with gentle shaking. Normal rabbit IgG was used as an NC. The 2% input reference was removed and stored at −20°C before antibody supplementation. The ChIP DNA was reverse crosslinked with 5 M NaCl and proteinase K at 65°C for 2 h, and then DNA was purified. Immunoprecipitated DNAs were amplified by PCR using their specific primers (Table 2). The primers of each PCR set, the sizes of PCR products, and annealing temperatures are listed in Table 3. In each PCR reaction, the corresponding inputs were taken in parallel for PCR validation. PCR products were resolved on a 3% agarose gel. Bands were visualized as described above for RT-PCR.

Quantization of Apoptosis by Flow Cytometry after Adding Dox

Cell apoptosis was quantified by annexin V-fluorescein isothiocyanate (FITC)/propidium iodide (PI) or annexin V-PE/7AAD staining (SouthernBiotech, Birmingham, AL, USA). Collected cells were washed twice with PBS and then stained with annexin V-FITC/PI or annexin V-PE/7AAD for 15 min according to the manufacturer's instructions. Then, cells were analyzed by flow cytometry (BD Biosciences) and apoptotic fractions were acquired.

Statistical Analysis

All data were expressed as the mean ± SD. Statistically significant differences between two groups were determined by a t test. For three or more groups, statistical analysis was performed using one-way ANOVA. $p < 0.05$ was considered as statistically significant.

SUPPLEMENTAL INFORMATION

Supplemental Information can be found online at https://doi.org/10.1016/j.omtn.2019.10.031.

AUTHOR CONTRIBUTIONS

Y.X. contributed to the experiment design, manuscript draft, and data analysis. J.G., S.S., X.L., and X.R. conducted the experiments, as well as processed the experimental data and drafted the manuscript. These four authors contributed equally to this article. J.Z., Y.L., L.L., J.M., and T.M. were involved in designing the study and drafting of this manuscript. L.S., D.W., and C.Y. were involved in carrying out data analyses.

CONFLICTS OF INTEREST

The authors declare no competing interests.

ACKNOWLEDGMENTS

This work is supported by grants from the Natural Science Foundation of China (81872503, 81872073, 81573010, and 81602725); China Postdoctoral Science Foundation (2019M661172); Liaoning Science and Technology Plan Project (2017225020 and 2015225007); Project of Key Laboratory of Neuro-oncology in Liaoning Province (112-2400017005); and a special developmental project guided by the central government of Liaoning Province (2017011553-301).

REFERENCES

1. Zhu, D., Tu, M., Zeng, B., Cai, L., Zheng, W., Su, Z., and Yu, Z. (2017). Up-regulation of miR-497 confers resistance to temozolomide in human glioma cells by targeting mTOR/Bcl-2. Cancer Med. *6*, 452–462.
2. Lefranc, F., Rynkowski, M., DeWitte, O., and Kiss, R. (2009). Present and potential future adjuvant issues in high-grade astrocytic glioma treatment. Adv. Tech. Stand. Neurosurg. *34*, 3–35.
3. Vogelbaum, M.A. (2018). Targeted therapies for brain tumors: will they ever deliver? Clin. Cancer Res. *24*, 3790–3791.
4. Ueno, M. (2007). Molecular anatomy of the brain endothelial barrier: an overview of the distributional features. Curr. Med. Chem. *14*, 1199–1206.
5. Takahashi, A., Kondoh, M., Kodaka, M., and Yagi, K. (2011). Peptides as tight junction modulators. Curr. Pharm. Des. *17*, 2699–2703.
6. Permuth, J.B., Chen, D.T., Yoder, S.J., Li, J., Smith, A.T., Choi, J.W., Kim, J., Balagurunathan, Y., Jiang, K., Coppola, D., et al. (2017). Linc-ing circulating long non-coding RNAs to the diagnosis and malignant prediction of intraductal papillary mucinous neoplasms of the pancreas. Sci. Rep. *7*, 10484.
7. Zhang, X., Sun, S., Pu, J.K., Tsang, A.C., Lee, D., Man, V.O., Lui, W.M., Wong, S.T., and Leung, G.K. (2012). Long non-coding RNA expression profiles predict clinical phenotypes in glioma. Neurobiol. Dis. *48*, 1–8.
8. Kogo, R., Shimamura, T., Mimori, K., Kawahara, K., Imoto, S., Sudo, T., Tanaka, F., Shibata, K., Suzuki, A., Komune, S., et al. (2011). Long noncoding RNA HOTAIR regulates polycomb-dependent chromatin modification and is associated with poor prognosis in colorectal cancers. Cancer Res. *71*, 6320–6326.
9. Ellis, B.C., Molloy, P.L., and Graham, L.D. (2012). CRNDE: a long non-coding RNA Involved in cancer, neurobiology, and development. Front. Genet. *3*, 270.
10. Chen, Y., Cao, K.E., Wang, S., Chen, J., He, B., He, G.U., Chen, Y., Peng, B., and Zhou, J. (2016). MicroRNA-138 suppresses proliferation, invasion and glycolysis in malignant melanoma cells by targeting HIF-1α. Exp. Ther. Med. *11*, 2513–2518.
11. Yamasaki, T., Seki, N., Yamada, Y., Yoshino, H., Hidaka, H., Chiyomaru, T., Nohata, N., Kinoshita, T., Nakagawa, M., and Enokida, H. (2012). Tumor suppressive microRNA-138 contributes to cell migration and invasion through its targeting of vimentin in renal cell carcinoma. Int. J. Oncol. *41*, 805–817.
12. Wang, W.H., Chen, J., Zhao, F., Zhang, B.R., Yu, H.S., Jin, H.Y., and Dai, J.H. (2014). miR-150-5p suppresses colorectal cancer cell migration and invasion through targeting MUC4. Asian Pac. J. Cancer Prev. *15*, 6269–6273.
13. Lu, W., Zhang, H., Niu, Y., Wu, Y., Sun, W., Li, H., Kong, J., Ding, K., Shen, H.M., Wu, H., et al. (2017). Long non-coding RNA linc00673 regulated non-small cell lung cancer proliferation, migration, invasion and epithelial mesenchymal transition by sponging miR-150-5p. Mol. Cancer *16*, 118.
14. Tulchinsky, E. (2000). Fos family members: regulation, structure and role in oncogenic transformation. Histol. Histopathol. *15*, 921–928.
15. Chinenov, Y., and Kerppola, T.K. (2001). Close encounters of many kinds: Fos-Jun interactions that mediate transcription regulatory specificity. Oncogene *20*, 2438–2452.
16. Eferl, R., Hasselblatt, P., Rath, M., Popper, H., Zenz, R., Komnenovic, V., Idarraga, M.H., Kenner, L., and Wagner, E.F. (2008). Development of pulmonary fibrosis through a pathway involving the transcription factor Fra-2/AP-1. Proc. Natl. Acad. Sci. USA *105*, 10525–10530.

17. Fernandes, K.A., Harder, J.M., Kim, J., and Libby, R.T. (2013). JUN regulates early transcriptional responses to axonal injury in retinal ganglion cells. Exp. Eye Res. *112*, 106–117.

18. Kharman-Biz, A., Gao, H., Ghiasvand, R., Zhao, C., Zendehdel, K., and Dahlman-Wright, K. (2013). Expression of activator protein-1 (AP-1) family members in breast cancer. BMC Cancer *13*, 441.

19. Bozec, A., Bakiri, L., Jimenez, M., Rosen, E.D., Catalá-Lehnen, P., Schinke, T., Schett, G., Amling, M., and Wagner, E.F. (2013). Osteoblast-specific expression of Fra-2/AP-1 controls adiponectin and osteocalcin expression and affects metabolism. J. Cell Sci. *126*, 5432–5440.

20. Engel, L., Gupta, B.B., Lorenzkowski, V., Heinrich, B., Schwerdtle, I., Gerhold, S., Holthues, H., Vollrath, L., and Spessert, R. (2005). Fos-related antigen 2 (Fra-2) memorizes photoperiod in the rat pineal gland. Neuroscience *132*, 511–518.

21. Roy, S., Khanna, S., Azad, A., Schnitt, R., He, G., Weigert, C., Ichijo, H., and Sen, C.K. (2010). Fra-2 mediates oxygen-sensitive induction of transforming growth factor beta in cardiac fibroblasts. Cardiovasc. Res. *87*, 647–655.

22. Zhou, L., Graves, M., MacDonald, G., Cipollone, J., Mueller, C.R., and Roskelley, C.D. (2013). Microenvironmental regulation of *BRCA1* gene expression by c-Jun and Fra2 in premalignant human ovarian surface epithelial cells. Mol. Cancer Res. *11*, 272–281.

23. He, J., Mai, J., Li, Y., Chen, L., Xu, H., Zhu, X., and Pan, Q. (2017). miR-597 inhibits breast cancer cell proliferation, migration and invasion through FOSL2. Oncol. Rep. *37*, 2672–2678.

24. Förster, C., Burek, M., Romero, I.A., Weksler, B., Couraud, P.O., and Drenckhahn, D. (2008). Differential effects of hydrocortisone and TNFα on tight junction proteins in an in vitro model of the human blood-brain barrier. J. Physiol. *586*, 1937–1949.

25. Huang, W., Eum, S.Y., András, I.E., Hennig, B., and Toborek, M. (2009). PPARα and PPARγ attenuate HIV-induced dysregulation of tight junction proteins by modulations of matrix metalloproteinase and proteasome activities. FASEB J. *23*, 1596–1606.

26. Cai, H., Liu, W., Xue, Y., Shang, X., Liu, J., Li, Z., Wang, P., Liu, L., Hu, Y., and Liu, Y. (2015). Roundabout 4 regulates blood-tumor barrier permeability through the modulation of ZO-1, Occludin, and Claudin-5 expression. J. Neuropathol. Exp. Neurol. *74*, 25–37.

27. Shen, S., Yu, H., Liu, X., Liu, Y., Zheng, J., Wang, P., Gong, W., Chen, J., Zhao, L., and Xue, Y. (2018). PIWIL1/piRNA-DQ593109 regulates the permeability of the blood-tumor barrier via the MEG3/miR-330-5p/RUNX3 axis. Mol. Ther. Nucleic Acids *10*, 412–425.

28. Lei, W., Wang, Z.L., Feng, H.J., Lin, X.D., Li, C.Z., and Fan, D. (2018). Long non-coding RNA SNHG12 promotes the proliferation and migration of glioma cells by binding to HuR. Int. J. Oncol. *53*, 1374–1384.

29. Ma, J., Wang, P., Yao, Y., Liu, Y., Li, Z., Liu, X., Li, Z., Zhao, X., Xi, Z., Teng, H., et al. (2016). Knockdown of long non-coding RNA MALAT1 increases the blood-tumor barrier permeability by up-regulating miR-140. Biochim. Biophys. Acta *1859*, 324–338.

30. Yu, H., Xue, Y., Wang, P., Liu, X., Ma, J., Zheng, J., Li, Z., Li, Z., Cai, H., and Liu, Y. (2017). Knockdown of long non-coding RNA XIST increases blood-tumor barrier permeability and inhibits glioma angiogenesis by targeting miR-137. Oncogenesis *6*, e303.

31. Chen, L., Xue, Y., Zheng, J., Liu, X., Liu, J., Chen, J., Li, Z., Xi, Z., Teng, H., Wang, P., et al. (2018). miR-429 regulated by endothelial monocyte activating polypeptide-II (EMAP-II) influences blood-tumor barrier permeability by inhibiting the expressions of ZO-1, occludin and claudin-5. Front. Mol. Neurosci. *11*, 35.

32. Shen, Y., Gao, X., Tan, W., and Xu, T. (2018). STAT1-mediated upregulation of lncRNA LINC00174 functions a ceRNA for miR-1910-3p to facilitate colorectal carcinoma progression through regulation of TAZ. Gene *666*, 64–71.

33. Miao, Y.S., Zhao, Y.Y., Zhao, L.N., Wang, P., Liu, Y.H., Ma, J., and Xue, Y.X. (2015). miR-18a increased the permeability of BTB via RUNX1 mediated down-regulation of ZO-1, occludin and claudin-5. Cell. Signal. *27*, 156–167.

34. Zhao, W., Wang, P., Ma, J., Liu, Y.H., Li, Z., Li, Z.Q., Wang, Z.H., Chen, L.Y., and Xue, Y.X. (2015). miR-34a regulates blood-tumor barrier function by targeting protein kinase Cε. Mol. Biol. Cell *26*, 1786–1796.

35. Zhou, Z.B., Du, D., Huang, G.X., Chen, A., and Zhu, L. (2018). Circular RNA Atp9b, a competing endogenous RNA, regulates the progression of osteoarthritis by targeting miR-138-5p. Gene *646*, 203–209.

36. Yang, R., Liu, M., Liang, H., Guo, S., Guo, X., Yuan, M., Lian, H., Yan, X., Zhang, S., Chen, X., et al. (2016). miR-138-5p contributes to cell proliferation and invasion by targeting Survivin in bladder cancer cells. Mol. Cancer *15*, 82.

37. Wang, Z., Yao, Y.J., Zheng, F., Guan, Z., Zhang, L., Dong, N., and Qin, W.J. (2017). Mir-138-5p acts as a tumor suppressor by targeting pyruvate dehydrogenase kinase 1 in human retinoblastoma. Eur. Rev. Med. Pharmacol. Sci. *21*, 5624–5629.

38. Sabre, L., Maddison, P., Sadalage, G., Ambrose, P.A., and Punga, A.R. (2018). Circulating microRNA miR-21-5p, miR-150-5p and miR-30e-5p correlate with clinical status in late onset myasthenia gravis. J. Neuroimmunol. *321*, 164–170.

39. Koshizuka, K., Hanazawa, T., Kikkawa, N., Katada, K., Okato, A., Arai, T., Idichi, T., Osako, Y., Okamoto, Y., and Seki, N. (2018). Antitumor *miR-150-5p* and *miR-150-3p* inhibit cancer cell aggressiveness by targeting *SPOCK1* in head and neck squamous cell carcinoma. Auris Nasus Larynx *45*, 854–865.

40. Liu, X.H., Sun, M., Nie, F.Q., Ge, Y.B., Zhang, E.B., Yin, D.D., Kong, R., Xia, R., Lu, K.H., Li, J.H., et al. (2014). Lnc RNA HOTAIR functions as a competing endogenous RNA to regulate HER2 expression by sponging miR-331-3p in gastric cancer. Mol. Cancer *13*, 92.

41. Wang, P., Liu, Y.H., Yao, Y.L., Li, Z., Li, Z.Q., Ma, J., and Xue, Y.X. (2015). Long non-coding RNA CASC2 suppresses malignancy in human gliomas by miR-21. Cell. Signal. *27*, 275–282.

42. Wang, R., Zhang, T., Yang, Z., Jiang, C., and Seng, J. (2018). Long non-coding RNA FTH1P3 activates paclitaxel resistance in breast cancer through miR-206/ABCB1. J. Cell. Mol. Med. *22*, 4068–4075.

43. She, K., Yan, H., Huang, J., Zhou, H., and He, J. (2018). miR-193b availability is antagonized by LncRNA-SNHG7 for FAIM2-induced tumour progression in non-small cell lung cancer. Cell Prolif. *51*, e12406.

44. Sun, X., Dai, G., Yu, L., Hu, Q., Chen, J., and Guo, W. (2018). miR-143-3p inhibits the proliferation, migration and invasion in osteosarcoma by targeting FOSL2. Sci. Rep. *8*, 606.

45. Reich, N., Maurer, B., Akhmetshina, A., Venalis, P., Dees, C., Zerr, P., Palumbo, K., Zwerina, J., Nevskaya, T., Gay, S., et al. (2010). The transcription factor Fra-2 regulates the production of extracellular matrix in systemic sclerosis. Arthritis Rheum. *62*, 280–290.

46. Maurer, B., Busch, N., Jüngel, A., Pileckyte, M., Gay, R.E., Michel, B.A., Schett, G., Gay, S., Distler, J., and Distler, O. (2009). Transcription factor Fos-related antigen-2 induces progressive peripheral vasculopathy in mice closely resembling human systemic sclerosis. Circulation *120*, 2367–2376.

47. Asano, Y. (2016). Recent advances in animal models of systemic sclerosis. J. Dermatol. *43*, 19–28.

48. Lewis, B.P., Burge, C.B., and Bartel, D.P. (2005). Conserved seed pairing, often flanked by adenosines, indicates that thousands of human genes are microRNA targets. Cell *120*, 15–20.

49. Yang, J.Z., Bian, L., Hou, J.G., and Wang, H.Y. (2018). miR-550a-3p promotes non-small cell lung cancer cell proliferation and metastasis through down-regulating TIMP2. Eur. Rev. Med. Pharmacol. Sci. *22*, 4156–4165.

50. Suo, H.B., Zhang, K.C., and Zhao, J. (2018). miR-200a promotes cell invasion and migration of ovarian carcinoma by targeting PTEN. Eur. Rev. Med. Pharmacol. Sci. *22*, 4080–4089.

51. Zhao, Y.Y., Zhao, L.N., Wang, P., Miao, Y.S., Liu, Y.H., Wang, Z.H., Ma, J., Li, Z., Li, Z.Q., and Xue, Y.X. (2015). Overexpression of miR-18a negatively regulates myocyte enhancer factor 2D to increase the permeability of the blood-tumor barrier via Krüppel-like factor 4-mediated downregulation of zonula occluden-1, claudin-5, and occludin. J. Neurosci. Res. *93*, 1891–1902.

52. Ciechomska, M., O'Reilly, S., Przyborski, S., Oakley, F., Bogunia-Kubik, K., and van Laar, J.M. (2016). Histone demethylation and Toll-like receptor 8-dependent cross-talk in monocytes promotes transdifferentiation of fibroblasts in systemic sclerosis via Fra-2. Arthritis Rheumatol. *68*, 1493–1504.

53. Wrann, C.D., Eguchi, J., Bozec, A., Xu, Z., Mikkelsen, T., Gimble, J., Nave, H., Wagner, E.F., Ong, S.E., and Rosen, E.D. (2012). FOSL2 promotes leptin gene expression in human and mouse adipocytes. J. Clin. Invest. *122*, 1010–1021.

54. Rani, A., Greenlaw, R., Runglall, M., Jurcevic, S., and John, S. (2014). *FRA2* is a STAT5 target gene regulated by IL-2 in human CD4 T cells. PLoS ONE *9*, e90370.

55. Zhou, W., Chen, X., Hu, Q., Chen, X., Chen, Y., and Huang, L. (2018). Galectin-3 activates TLR4/NF-κB signaling to promote lung adenocarcinoma cell proliferation through activating lncRNA-NEAT1 expression. BMC Cancer *18*, 580.

56. Feldstein, O., Nizri, T., Doniger, T., Jacob, J., Rechavi, G., and Ginsberg, D. (2013). The long non-coding RNA ERIC is regulated by E2F and modulates the cellular response to DNA damage. Mol. Cancer *12*, 131.

57. Wang, J., and Sun, G. (2017). FOXO1-MALAT1-miR-26a-5p feedback loop mediates proliferation and migration in osteosarcoma cells. Oncol. Res. *25*, 1517–1527.

58. Teng, H., Wang, P., Xue, Y., Liu, X., Ma, J., Cai, H., Xi, Z., Li, Z., and Liu, Y. (2016). Role of HCP5-miR-139-RUNX1 feedback loop in regulating malignant behavior of glioma cells. Mol. Ther. *24*, 1806–1822.

59. Zhao, X., Liu, Y., Zheng, J., Liu, X., Chen, J., Liu, L., Wang, P., and Xue, Y. (2017). GAS5 suppresses malignancy of human glioma stem cells via a miR-196a-5p/FOXO1 feedback loop. Biochim Biophys Acta Mol Cell Res *1864*, 1605–1617.

OMTN, Volume *18*

Supplemental Information

Role of linc00174/miR-138-5p (miR-150-5p)/FOSL2 Feedback Loop on Regulating the Blood-Tumor Barrier Permeability

Jizhe Guo, Shuyuan Shen, Xiaobai Liu, Xuelei Ruan, Jian Zheng, Yunhui Liu, Libo Liu, Jun Ma, Teng Ma, Lianqi Shao, Di Wang, Chunqing Yang, and Yixue Xue

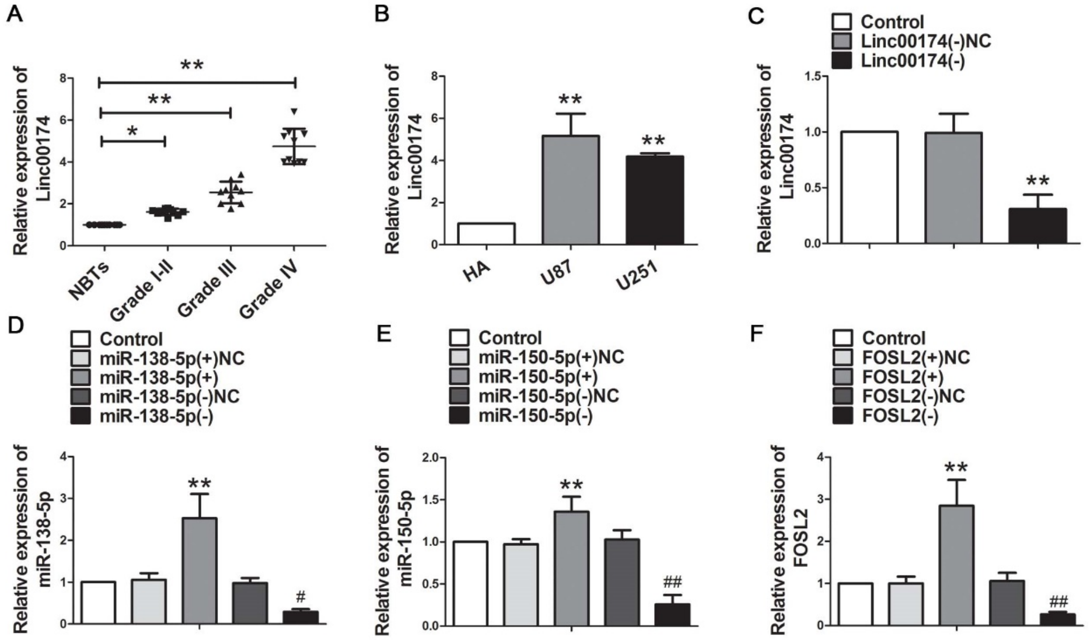

Supplementary Figure 1. Expression of Linc00174 in glioma tissues and cells, as well as the transfection efficiency of Linc00174, miR-138-5p, miR-150-5p and FOSL2

(A) Relative expression of Linc00174 in glioma tissues with different grades and normal brain tissues (NBTs). Data represented mean ± SD (n = 10, each). *P < 0.05 and **P < 0.01 vs. NBTs group. (B) Expression of Linc00174 in glioma cells with U87 and U251. Data represented mean ± SD (n = 3, each). **P < 0.01 vs. HA group. (C) The expression of linc00174 levels after linc00174 knockdown. Data represented mean ± SD (n = 3, each). **P < 0.01 vs. Linc00174(-) group. (D, E) Relative expression of miR-138-5p or miR-150-5p was detected by qRT-PCR after overexpression and inhibition of miR-138-5p or miR-150-5p in GECs. Data represented mean ± SD (n = 3, each), **P < 0.01 vs. miR-138-5p(+)NC and #P < 0.05 vs. miR-138-5p(-)NC. **P < 0.01 vs. miR-150-5p(+)NC and ##P < 0.05 vs. miR-150-5p(-)NC. (F) The relative expression of FOSL2 was detected by qRT-PCR after stabled transfection of FOSL2(+) or FOSL2(-) and FOSL-NC. Data represented mean ± SD ($n = 3$, each), $^{**}P < 0.01$ vs. FOSL2(+)NC and $^{##}P < 0.05$ vs. FOSL2(-)NC.